UNIVERSITY OF CALIFORNIA SAN DIEGO

Localization of NADH Shuttling Proteins Implicated in Peroxisome Biogenesis in *Pichia pastoris*

A thesis submitted in partial satisfaction of the requirements
for the degree of Master of Science

in

Biology

by

Paul Li

Committee in charge:

Professor Suresh Subramani, Chair
Professor James Kadonaga
Professor Immo Scheffler

2020

The thesis of Paul Li is approved, and it is acceptable in quality and form for publication on microfilm and electronically:

_____

_____

_____

Chair

University of California San Diego

2020

TABLE OF CONTENTS

LIST OF FIGURES

LIST OF TABLES

ACKNOWLEDGEMENTS

I would like to thank Dr. Suresh Subramani for giving me the opportunity to do research through the BS/MS program. Thank you for always giving helpful feedback during lab meetings and helping me with the presentation and thesis. I would also like to thank Dr. Jean-Claude Farré for designing and helping me with my experiments and for giving me constructive feedback on my presentation and thesis. Thank you for your constant support and encouragement. I really appreciate the time you take out of your day to help me understand the big picture of my experiments. I came in with zero lab experience and I learned not only lab techniques, but also the importance of being able to think critically about science. Finally, I would like to thank my friends and family who have always been there for me.

Chapter 1 is co-authored with Farré, Jean-Claude. The thesis author was the primary author of this chapter.

ABSTRACT OF THE THESIS

Localization of NADH Shuttling Proteins Implicated in Peroxisome Biogenesis in *Pichia pastoris*

by

Paul Li

Master of Science in Biology

University of California San Diego, 2020

Professor Suresh Subramani, Chair

Peroxisomes proliferate in media whose utilization requires peroxisomal metabolic pathways. In methylotrophic yeast, such as *Pichia pastoris*, oleate and methanol are the most common carbon sources used for peroxisome proliferation studies. When grown in these conditions, peroxisome metabolism is essential for carbon assimilation and energy production. In

Saccharomyces cerevisiae, during growth in oleate, NADH shuttling from the peroxisome to mitochondria, via the cytosol, maintains the cellular redox balance during fatty acid β-oxidation and contributes to energy production. In *P. pastoris*, during growth in methanol, NADH produced by methanol oxidation shuttles to the mitochondria becoming the only source of energy; however, the NADH shuttling mechanism, which typically requires enzymes in peroxisomes, cytosol and mitochondria, has not been studied yet in this yeast. We used fluorescence microscopy to determine the subcellular localization of the homologous *P. pastoris* NADH shuttling proteins (malate dehydrogenases and glycerol 3-phosphate dehydrogenases). Surprisingly, none of the NADH shuttling proteins fused to GFP showed peroxisomal localization, although this was expected. To improve the detection, we developed a divergent bimolecular fluorescence complementation (BiFC) assay to detect low levels of peroxisomally localized proteins which could be masked by a strong cytosolic localization. Using this assay, we confirmed that one of the malate dehydrogenases has a dual localization, cytosolic and peroxisomal, but only when grown in oleate, but it was exclusively cytosolic when grown in methanol. These localizations can be rationalized in terms of the NADH produced by oleate metabolism in the peroxisome matrix and in the cytosol during methanol metabolism. Finally, we elucidated the pathway responsible for targeting the malate dehydrogenase to the peroxisome; however, no obvious peroxisomal targeting signal was found in the enzyme suggesting an alternative translocation mechanism, such as piggyback import with a peroxisomal protein containing a peroxisomal targeting signal.

Introduction

Peroxisomes are single membrane bound organelles that have many functions, such as fatty acid metabolism and reactive oxygen species (ROS) detoxification. In methylotrophic yeast, peroxisomes are also important for methanol metabolism (van der Klei et al., 2006). In mammals, in addition to fatty acid metabolism, peroxisomes play a role in cholesterol biosynthesis, bile acid synthesis, and amino acid catabolism (Wanders et al., 2016). Notably deficiencies in peroxisomal metabolic pathways or in biogenesis cause peroxisome biogenesis disorders in humans.

Peroxisomes may form through *de novo* biogenesis or through growth and division. In the *de novo* biogenesis model, peroxisomes are formed through the fusion of pre-peroxisomal vesicles derived from the ER from which peroxisomal membrane proteins (PMPs) were inserted into the ER and sorted into the pre-peroxisomal vesicles (Agrawal & Subramani, 2013; Farré et al., 2019). In the growth and division model, peroxisomes form from pre-existing peroxisomes receiving lipids from the ER during growth before division (Motley & Hettema, 2007). In this model, instead of PMP insertion via the ER, PMPs are synthesized in the cytosol and directly inserted into the peroxisome membrane. Under the growth and division model, existing peroxisomes will elongate and constrict before undergoing fission.

Cargo imported into the peroxisome

Once peroxisomes form and have the full complement of peroxisomal membrane proteins, including the protein translocation machinery, they become import competent and can import cargo into the peroxisomal matrix. Since peroxisomes do not have their own DNA or translational machinery, peroxisomal matrix proteins are encoded by nuclear genes and synthesized by polyribosomes in the cytosol before import into the peroxisomal matrix. Peroxisomal matrix

proteins are imported into the peroxisome through the use of peroxisomal targeting signal (PTS) 1 or PTS2 (Figure 1). Cargos imported by the PTS1 pathway have a PTS at the C-terminus, in the form of a conserved tripeptide (S/A/C), (K/R/H), and (L/M), with Serine-Lysine-Leucine, or SKL, being the most common form (Gould et al., 1989; Brocard & Hartig, 2006). Cargos imported through the PTS2 pathway have a PTS near the N-terminus in the form of a nonapeptide, (R/K)-(L/V/I)-$(X)_5$-(H/Q)-(L/A) or (R/K)-(L/V/I/Q)-X-X-(L/V/I/H/Q)-(L/S/G/A/K)-X-(H/Q)-(L/A/F) (Kunze et al., 2015). Thiolase, an important enzyme involved in the β-oxidation of fatty acids, is a known peroxisomal protein in yeast with a PTS2 sequence at the N-terminus that is targeted to the peroxisome by the PTS2 pathway (Erdmann, 1994). Cargo receptors, such as the PTS1 receptor encoded by the *PEX5* gene and the PTS2 receptor encoded by the *PEX7* gene recognize and bind to PTS1 and PTS2, respectively (Elgersma et al.,1998; Farré et al., 2019). The PTS receptor and cargo complex then translocates and docks at the docking complex on the peroxisomal membrane consisting of Pex13, Pex14, and Pex17 (Figure 1). Pex14, a translocon component, is required for the PTS receptors to dock on the peroxisomal membrane for import of the PTS receptor and PTS-containing cargo. Once the PTS receptor and PTS-containing cargo complex are imported, the PTS receptor dissociates from the cargo and recycles back to the cytosol to bring in more PTS-containing cargo (Ma et al., 2011). Peroxisomes that have peroxisomal membrane proteins but lack some or all peroxisomal matrix proteins are called peroxisomal ghosts or remnants, such as in *pex* mutants, Δ*pex5*, Δ*pex7*, and Δ*pex14*.

Some enzymatic functions present in the peroxisomal matrix are also required in other compartments and nature has found different mechanisms to fulfill this purpose. Some examples of these mechanisms include gene duplication, protein modification, piggybacking, readthrough

extension, alternative start sites of transcription, or alternative splicing. In *S. cerevisiae*, the different isoforms, including the peroxisomal isoform, of malate dehydrogenases are encoded by

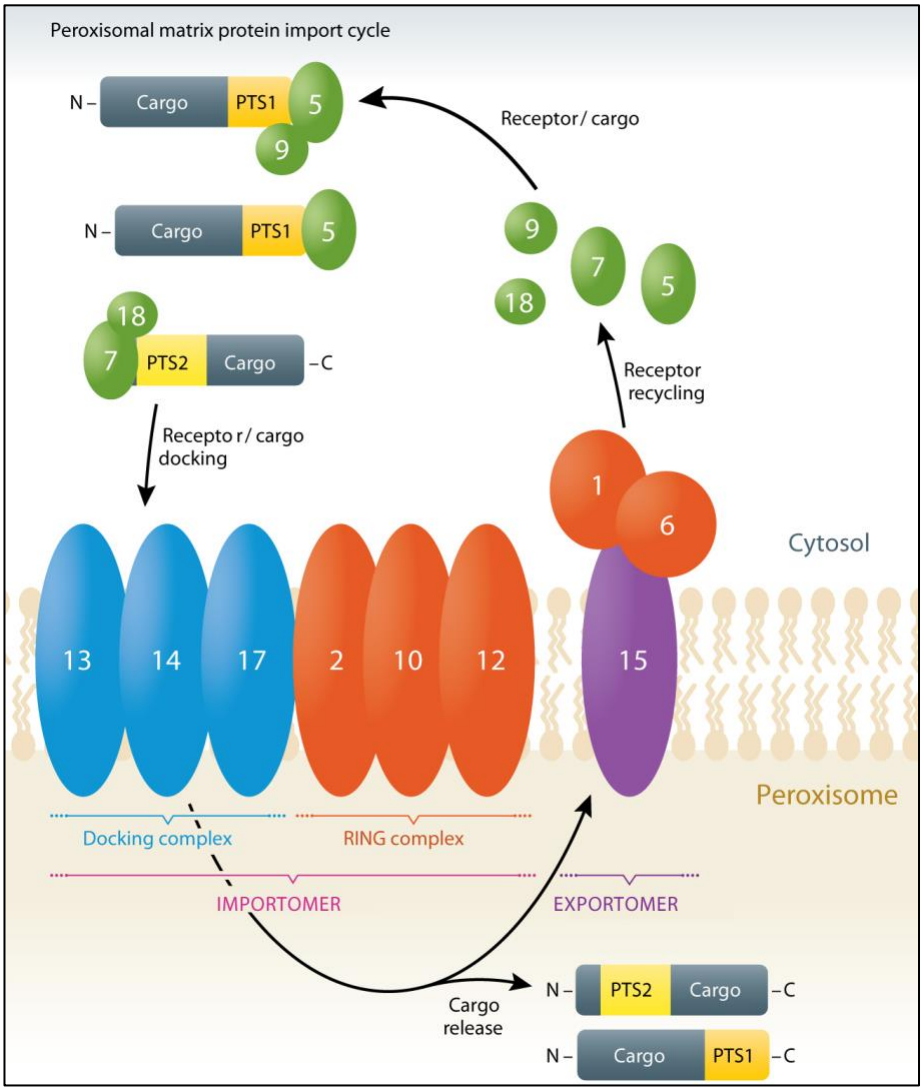

Figure 1. Peroxisomal matrix protein import cycle. The import cycle is composed of an importomer that includes the docking complex (Pex13, Pex14, and Pex17) and ring complex (Pex2, Pex10, Pex12), and an exportomer (Pex15, Pex1, and Pex6). The PTS1 at the C-terminus of cargo is recognized by the PTS1 receptor (Pex5) and the PTS2 at the N-terminus is recognized by the PTS2 receptor (Pex7). PTS receptors bind to the PTS-containing cargo and dock at the peroxisomal membrane through Pex14 that is essential for peroxisomal import. The PTS receptors release the cargo upon import and are recycled back to the cytosol for more peroxisomal matrix protein import. Pex9 is a PTS1 co-receptor and Pex18 is a PTS2 co-receptor (Adapted from Farré et al., 2019).

separate genes as a result of gene duplication and the peroxisomal isoform of Gpd1 is regulated by phosphorylation. *Sc*Pnc1, a protein that does not possess a PTS can piggyback on *Sc*Gpd1, a known

PTS2-containing protein, into the peroxisome (Kumar et al., 2016). *Sc*YCAT produces mitochondrial and peroxisomal isoforms through alternative start sites of transcription (Elgersma et al., 1995). In mammals, lactate dehydrogenase B (LDHBx) and malate dehydrogenase extended (MDHx) both have a PTS1 motif uncovered by translational readthrough, coding past the stop codon and extending the length of the protein (Hofhuis et al., 2016; Schueren et al., 2014). The cytosolic signal for both proteins had to be reduced for visualization of the peroxisomal isoforms. Both LDHBx and MDHx have UGA as the stop codon followed by CUA, with the stop codon context or amino acids following the stop codon increasing the likelihood of translational readthrough. UGA has the most efficient readthrough, while UAA has the least efficient readthrough. UGA in combination with CUA has been shown to have an efficient ribosomal readthrough in lower and higher eukaryotes (Stiebler et al., 2014). In lower eukaryotes such as fungi, readthrough extension exposing a PTS1 has also been observed in *U. maydis* for phosphoglycerate kinase and triose phosphate isomerase (Ast et al., 2013). In *Y. lipolytica*, peroxisomal and cytosolic isoforms of malate dehydrogenase (MDH2) are generated through alternative splicing (Kabran et al., 2012). Our interest, therefore, was to find out which of these mechanisms is used in *P. pastoris* to deliver homologous NADH shuttling proteins into multiple subcellular compartments.

β-oxidation in yeast and higher eukaryotes

In higher eukaryotes, fatty acids are oxidized in the peroxisome and mitochondria. The steps of β-oxidation (dehydrogenation, hydration, oxidation, and thiolysis) in peroxisomes are conserved in most organisms and even the human enzymes of β-oxidation have been reconstituted in *S. cerevisiae* showing the differences in fatty acid substrate specificities between human and

yeast (Knoblach & Rachubinski, 2018). In mammals, β-oxidation occurs in both peroxisomes and mitochondria. The peroxisome is responsible for the oxidation of very long-chain fatty acids, and the mitochondria oxidizes short-chain fatty acids and also performs the final oxidation step (Wanders et al., 2016). The shortened fatty acids produced in the peroxisome traffic to the mitochondria through the carnitine shuttle (Poirier et al., 2006; Wanders et al., 2016). In plants and yeast, fatty acids are fully oxidized in the peroxisome. *S. cerevisiae* has a broad range of specificity for saturated and unsaturated fatty acids as the substrate for peroxisomal β-oxidation (Roermund et al., 2003; Hiltunen et al., 2003).

Peroxisome metabolism in *P. pastoris* and *S. cerevisiae*

Peroxisomes can grow and divide under peroxisome proliferating conditions when media such as methanol or oleate are used. Cargos important for methanol and oleate metabolism will be imported into the peroxisome through the PTS1 and PTS2 pathways. *P. pastoris* is a methylotrophic yeast that can metabolize and grow on a methanol as a sole carbon source (Figure 2). In this yeast, under methanol conditions, peroxisomes proliferate and important peroxisomal matrix enzymes, such as alcohol oxidases (Aox1 and Aox2), catalase (Cat1), and dihydroxyacetone synthase (Das1 and Das2) are imported into the peroxisome through the PTS1 pathway (Van der Klei et al., 2006). The compartmentalization of these peroxisomal enzymes is important for methanol metabolism and growth in methanol media (Van der Klei et al., 2006).

In the peroxisome, alcohol oxidase initially breaks down methanol into formaldehyde and hydrogen peroxide, both harmful substances to the cell. Catalase oxidizes hydrogen peroxide into oxygen and water in the peroxisome. Some formaldehyde in the peroxisome will diffuse into the cytosol for NADH production by formaldehyde dehydrogenase (Fld1) and formate dehydrogenase

(Fdh1) for energy, while another portion in the peroxisome will be converted into glyceraldehyde 3-phosphate and dihydroxyacetone phosphate for carbon assimilation (Van der Klei et al., 2006; Vogl et al., 2016). Unlike *P. pastoris*, *S. cerevisiae* is unable to metabolize methanol because it lacks alcohol oxidases (Distel et al., 1987; Veenhuis et al., 1983) and is subject to gene repression and methanol toxicity (Yasokawa et al., 2010). In the absence of Pex5, alcohol oxidases of methylotrophic yeasts are not imported into the peroxisome and growth in methanol medium is impaired, while thiolase, which uses the PTS2 pathway, can still be imported in methanol or oleate in Δ*pex5* cells and consequently growth in oleate medium is unaffected (McCollum et al., 1993).

Both *P. pastoris* and *S. cerevisiae* can metabolize and grow on oleate as a single carbon source. In the absence of Pex7, growth on oleate is impaired because PTS2-containing, peroxisomal enzymes required for oleate metabolism are mislocalized to the cytosol, while growth in methanol (in methylotrophic yeast) is unaffected (Elgersma et al., 1998). Specifically, thiolase, a PTS2-containing enzyme participating in the β-oxidation in peroxisomes, is not imported into peroxisomes in Δ*pex7* cells (McCollum et al., 1993).

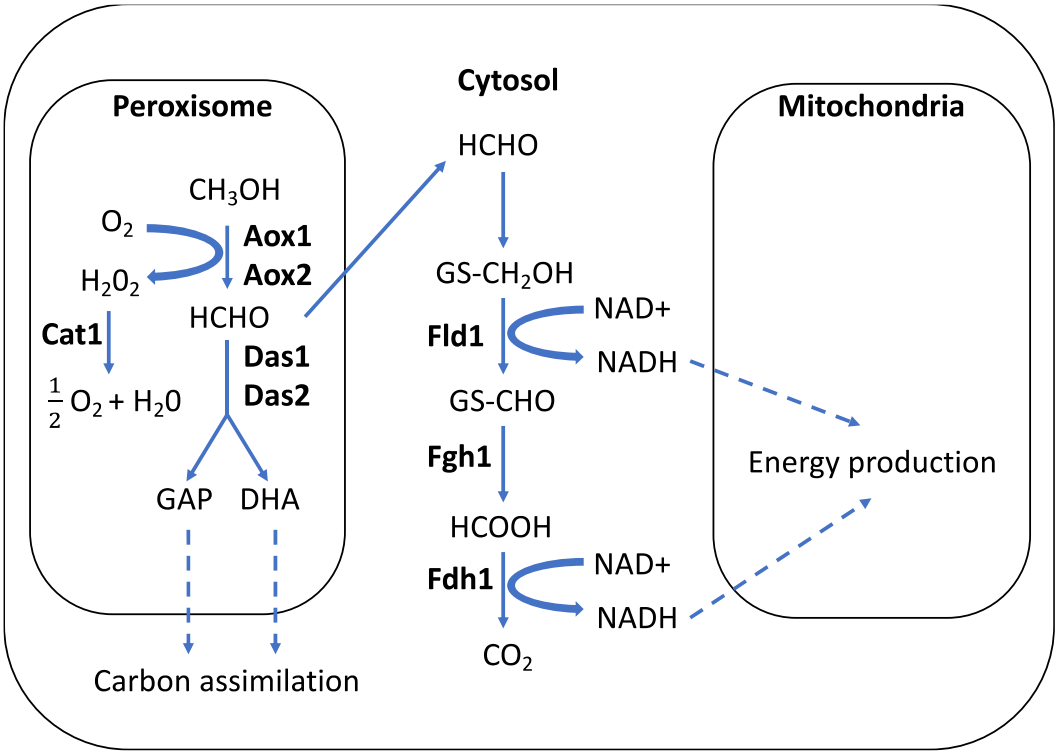

Figure 2. Overview of methanol metabolism and NADH shuttling in methylotrophic yeast (*P. pastoris*). Methanol (CH_3OH) is broken down into formaldehyde (HCHO) by alcohol oxidase (Aox1 and Aox2) and hydrogen peroxide (H_2O_2) is degraded by catalase (Cat1). Formaldehyde diffuses into the cytosol and subsequent reactions produce NADH for energy from methanol metabolism. Some formaldehyde is also converted inside peroxisomes into GAP and DHA that can undergo carbon assimilation. Das1 and Das2, dihydroxyacetone synthase; DHA, dihydroxyacetone; GAP, glyceraldehyde 3-phosphate, Fld1, formaldehyde dehydrogenase; Fgh1, s-formylgluthathione hydrolase; Fdh1, formate dehydrogenase (Adapted from Vogl et al., 2016).

NADH shuttling proteins implicated in peroxisome biogenesis in *S. cerevisiae*

During growth in oleate or methanol as a sole carbon source, yeast obtain their carbon and energy sources by metabolizing these substrates. The peroxisomal β-oxidation of fatty acids consumes NAD^+, yielding NADH, which needs to shuttle out of the peroxisome to maintain a peroxisomal redox balance. Once NADH is in the cytosol, it shuttles to the mitochondria and is subsequently transferred to complex I in the electron transport chain, contributing to the production of ATP. As described earlier, methanol metabolism does not produce intraperoxisomal NADH, but the oxidation of formaldehyde, a product of the methanol metabolism, reduces NAD^+, yielding 2 NADH, which shuttle to mitochondria for ATP production as well (Figure 2).

Most of the NAD+/NADH shuttling studies from peroxisome to mitochondria have been done in *S. cerevisiae*. In baker's yeast, malate dehydrogenase (MDH) and glycerol 3-phosphate dehydrogenase (GPD) are both involved in redox balance in regenerating peroxisomal NAD+ during peroxisome metabolism (Figure 3) (Al-Saryi et al., 2017). Malate dehydrogenase converts oxaloacetate to malate and vice-versa, while glycerol 3-phosphate dehydrogenase converts DHAP into glycerol 3-phosphate reversibly. *S. cerevisiae* has three isozymes of MDH and two isozymes of GPD that participate in the shuttle that transports NADH between subcellular compartments, as NADH is impermeable to organelle membranes (Steffan & McAlister-Henn, 1992; Roermund et al., 1995).

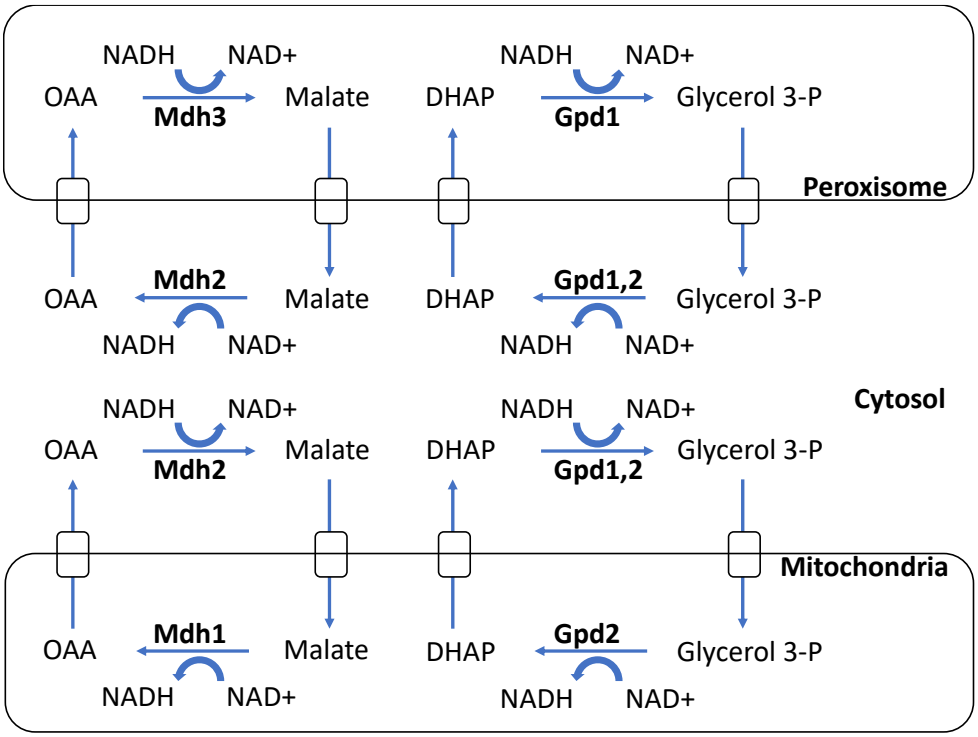

Figure 3. Overview of NADH shuttling during growth in oleate in *S. cerevisiae*. NADH shuttles out of the peroxisome through the malate and glycerol 3-phosphate shuttles. Mdh3 and Gpd1 shuttle NADH from the peroxisome to the cytosol, regenerating NAD+. Mdh2 and Gpd1, 2 can regenerate NADH in the cytosol. They then shuttle NADH from the cytosol to the mitochondria. Mdh1 regenerates the NADH in the mitochondria that originates from fatty acid metabolism in the peroxisome. Glycerol 3-P: glycerol 3-phosphate; OAA: oxaloacetate; DHAP: dihydroxyacetone phosphate (Adapted from Al-Saryi et al., 2017; Bakker et al., 2001).

Mdh3 is a homodimeric, peroxisomal isozyme (Moriyama et al., 2018) and oxidizes NADH generated from fatty acid oxidation back to NAD+ through the conversion of oxaloacetate

to malate and shuttles the reducing equivalents from the peroxisome to the cytosol in the form of metabolites such as malate that can be transported across the membrane. Mdh3 has a PTS1, SKL, at its C-terminus that targets it to peroxisomes (Steffan & McAlister-Henn, 1992; Elgersma et al., 1996). Mdh3 is required for β-oxidation and growth in oleate medium (Roermund et al., 1995). Mdh3 is involved in intraperoxisomal redox balance but is not involved in the glyoxylate cycle as growth on acetate is not impaired in Δ*mdh3* cells (Al-Saryi et al., 2017; Roermund et al., 1995; Kunze & Hartig, 2013).

Mdh2 is a cytosolic isozyme that converts malate back to oxaloacetate regenerating NADH transported from the peroxisome. Mdh2 may also convert oxaloacetate to malate, as aspartate is shuttled from the mitochondria to the cytosol through the malate aspartate shuttle and then converted to oxaloacetate that can serve as a substrate for conversion back to malate (Bakker et al., 2001; Palmieri et al., 2006; Cavero et al., 2003). Mdh2 plays a role in gluconeogenesis by providing oxaloacetate as a substrate and participates in the glyoxylate cycle as supported by a growth defect in ethanol or acetate in Δ*mdh2* cells (Kunze et al., 2006; Minard & McAlister-Henn, 1991). Like many gluconeogenic enzymes, Mdh2 undergoes degradation in glucose medium. The first proline from the N-terminus of Mdh2 targets Mdh2 for degradation through the Pro/N-end rule pathway in the presence of excess glucose (Minard & McAlister-Henn, 1992; Chen et al., 2017).

Mdh1, the mitochondrial isozyme, regenerates the NADH that was produced from fatty acid metabolism or glucose metabolism by the conversion of malate to oxaloacetate (Thompson & McAlister-Henn,1989; Minard & McAlister-Henn,1991; Pines et al., 1997). Mdh1 regenerates the NADH that was transported from the cytosol to the mitochondria, including NADH generated from β-oxidation that was shuttled from the peroxisome to the cytosol. Mdh1 has a mitochondrial

presequence at the N-terminus and plays a role in the TCA cycle (McAlister-Henn & Thompson, 1987).

Gpd1 exists as a peroxisomal pool containing a PTS2 sequence at the N-terminus and a cytosolic pool, while Gpd2 has mitochondrial and cytosolic pools. Peroxisomal localization of Gpd1 is regulated by phosphorylation at S24 and S27 and is dependent on Pex7 (Jung et al., 2009; Oeljeklaus et al., 2016). Cytosolic and nuclear localization of Gpd1 usually occurs under osmotic stress conditions such as oleate and high salt medium. Gpd is involved in glycerol synthesis and responds to hyperosmotic conditions by producing glycerol to maintain osmotic balance within the cell (Jung et al., 2010; Lee et al., 2012). In Δ*gpd1* cells, mutants showed growth impairments in glucose medium and 1M NaCl mimicking hyperosmostic conditions (Al-Saryi et al., 2017). Δ*gpd1* did not show growth impairment in oleate, while the Δ*mdh3* mutant alone and the double mutant Δ*gpd1* Δ*mdh3* exhibited a growth impairment in oleate medium (Al-Saryi et al., 2017; Roermund et al., 1995). Gpd2 has a mitochondrial presequence at the N-terminus and may be involved in the intramitochondrial redox balance of NAD^+/NADH (Valadi et al., 2004).

Chapter 1: Characterization of NADH Shuttling Homologs in *P. pastoris*

1) NADH shuttling proteins in *P. pastoris*

In the methylotrophic yeast, *P. pastoris,* none of these shuttling mechanisms that transport NADH have been described and the proteins responsible have not been identified. In *S. cerevisiae* the three malate dehydrogenases have a strong sequence similarity between them, and the most significant differences are the presence of a mitochondrial or a peroxisomal targeting signal (Figure 4A). Similarly, the two glycerol-3-phosphate dehydrogenases share a strong protein sequence homology and one of them has a peroxisomal targeting signal (Figure 4B). To identify the *P. pastoris* counterpart of these dehydrogenases, we searched the *P. pastoris* GS115 database

performing a protein-protein BLAST (BLASTP) using the three isoforms of MDH and two isoforms of GPD from *S. cerevisiae* as query, and we found *P. pastoris* has two isoforms of MDH and only one isoform of GPD (Figure 4A and 4B). Since we did not know which isoforms in *P. pastoris* correspond to those in *S. cerevisiae*, we referred to them as *Pp*MdhA, *Pp*MdhB, and *Pp*GpdA.

A

Figure 4. Sequence homologies between dehydrogenases implicated in NADH shuttling in *P. pastoris* and *S. cerevisiae*. A) Malate dehydrogenases for *S. cerevisiae* (NP_012838.1, NP_014515.2, and NP_010205.1) and *P. pastoris* (XP_002491128.1 and XP_002494265.1). **B)** Glycerol 3-phosphate dehydrogenases for *S. cerevisiae* (NP_010262.1 and NP_014582.1) and *P. pastoris* (XP_002492095.1). Protein sequences were aligned using the Clustal Omega Multiple Clustal Alignment. * identity ; . and : similarity. Mitochondrial pre-sequences are highlighted in red and peroxisomal targeting signals are depicted in green.

B

```
ScGpd1    ------------------------------------------------MSAAARLNLTS    12
ScGpd2    MLAVRRLTRYTFLKRTHPVLYTRRAYKILPSRSTFLRRSLLQTQLHSKMTAHTNIKQHKH    60
PpGpdA    -------------------MYLTSTVRALPVH--F-------------------FRSRH    19
                                                                  .

ScGpd1    GHINAGRKRSSSS-VSLKAAEKPFKVTVIGSGNWGTTIAKVVAENCKGYPEVFAPIVQMW    71
ScGpd2    CHEDHPIRRSDSAVSIVHLKRAPFKVTVIGSGNWGTTIAKVIAENTELHSHIFEPEVRMW   120
PpGpdA    CIRTM--SNIVEKKQSEFSRAEPFRVAVIGSGNWGTTVAKIIAENTNERPEEFVRDVNMW    77
                    .  .          **:*:**********:**::*** :   . *   *.**

ScGpd1    VFEEEINGEKLTEIINTRHQNVKYLPGITLPDNLVANPDLIDSVKDVDIIVFNIPHQFLP   131
ScGpd2    VFDEKIGDENLTDIINTRHQNVKYLPNIDLPHNLVADPDLLHSIKGADILVFNIPHQFLP   180
PpGpdA    VYEEDIEGRKLTDIINEEHENVKYLPGVKLPKNLHATPDLLAVASPADILVFNVPHQFLS   137
          *::*.* ..:**:*** .*:******.: **.** * ***:   . .**:***:*****

ScGpd1    RICSQLKGHVDSHVRAISCLKGFEVGAKGVQLLSSYITEELGIQCGALSGANIATEVAQE   191
ScGpd2    NIVKQLQGHVAPHVRAISCLKGFELGSKGVQLLSSYVTDELGIQCGALSGANLAPEVAKE   240
PpGpdA    RILQQLKGKIKPTARAISCLKGLNVEKNSCQLLSTQIENELNIHCGVLSGANLAPEIARE   197
          .* .**:*::   .********:::  :. ****: : :**.*:**.*****:* *:*:*

ScGpd1    HWSETTVAYHIPKDFRGEGKDVDHKVLKALFHRP-YFHVSVIEDVAGISICGALKNVVAL   250
ScGpd2    HWSETTVAYQLPKDYQGDGKDVDHKILKLLFHRP-YFHVNVIDDVAGISIAGALKNVVAL   299
PpGpdA    CWSETTIAYVKPKDYRGKYDDVTPFTIKHLFHRPAYFHVQVIEDIAGASLGGALKNVIAL   257
           *****:**  ***::*. .**    :* ***** ****.**:*:** *: ******:**

ScGpd1    GCGFVEGLGWGNNASAAIQRVGLGEIIRFGQMFFPESREETYYQESAGVADLITTCAGGR   310
ScGpd2    ACGFVEGMGWGNNASAAIQRLGLGEIIKFGRMFFPESKVETYYQESAGVADLITTCSGGR   359
PpGpdA    AVGFVDGLNWGDNAKGAIIRLGLREMIHFGHTYFPGAKSYTLTCESAGAADLITSCAGGR   317
          . ***:*:.**:**..** *:** *:*:**: :** ::  *   ****.*****:*:***

ScGpd1    NVKVARLMATSGKDAWECEKELLNGQSAQGLITCKEVHEWLETCGSVEDFPLFEAVYQIV   370
ScGpd2    NVKVATYMAKTGKSALEAEKELLNGQSAQGIITCREVHEWLQTCELTQEFPLFEAVYQIV   419
PpGpdA    NFKVGREIAATGKPAEQVEAELLNGQSAQGIITAAEVYEFLSSKGDLNSYPLLITVYLIL   377
          *.**.  :* :** * : * **********:**. **:*:*.:    :.:**: :** *:

ScGpd1    YNNYPMKNLPDMIEELDLHED---   391
ScGpd2    YNNVRMEDLPEMIEELDIDDE---   440
PpGpdA    KGERSAECIPEYFNKTEDVKHWED   401
           .:   : :*: ::: :  ..
```

Figure 4, Continued. Sequence homologies between dehydrogenases implicated in NADH shuttling in *P. pastoris* and *S. cerevisiae*. A) Malate dehydrogenases for *S. cerevisiae* (NP_012838.1, NP_014515.2, and NP_010205.1) and *P. pastoris* (XP_002491128.1 and XP_002494265.1). **B)** Glycerol 3-phosphate dehydrogenases for *S. cerevisiae* (NP_010262.1 and NP_014582.1) and *P. pastoris* (XP_002492095.1). Protein sequences were aligned using the Clustal Omega Multiple Clustal Alignment. * identity ; . and : similarity. Mitochondrial pre-sequences are highlighted in red and peroxisomal targeting signals are depicted in green.

We analyzed the *P. pastoris* NADH shuttling proteins sequences manually and using the PTS1 predictor (http://mendel.imp.ac.at/pts1/), but no obvious SKL at the C-terminus or any variation of the consensus sequence was found (Table 1). A PTS score equal to or greater than 0 would potentially have a predictable PTS1, while a PTS score under -10 would not have a predictable PTS1 (Neuberger et al., 2003). Based on this scoring system, all of the Mdh and Gpd proteins listed for *P. pastoris* and *S. cerevisiae* scored below -10 and do not have a predictable PTS1, except for *Sc*Mdh3 that has a PTS score above 0 and has an SKL as the PTS1 at the C-terminus (Table 1).

When analyzing the N-terminus of the NADH shuttling protein homologs, no PTS2 sequences corresponding to the consensus sequences (R/K)-(L/V/I)-$(X)_5$-(H/Q)-(L/A) or (R/K)-(L/V/I/Q)-X-X-(L/V/I/H/Q)-(L/S/G/A/K)-X-(H/Q)-(L/A/F) were found using EMBOSS fuzzpro that can search for the different combinations of the consensus sequences. Only *Sc*Gpd1 has a PTS2 at the N-terminus with the consensus sequence (RLNLTSGHL) (Figure 4B). The closest PTS2 consensus near the N-terminus had a match of 6 out of 9 amino acids for GpdA, MdhA, and MdhB (Figure 5). It has been shown that phosphorylation of serines near the PTS2 of *Sc*Gpd1 regulates peroxisomal localization, so we indicated predicted phosphorylation sites surrounding each potential PTS2 (Ast et al., 2013).

Figure 5. PTS2 sequence analysis of *P. pastoris* NADH shuttling dehydrogenases.
The PTS2 consensus sequence (R/K)-(L/V/I/Q)-X-X-(L/V/I/H/Q)-(L/S/G/A/K)-X-(H/Q)-(L/A/F) used to search for a potential PTS2 is in red and amino acids in the protein that fit the PTS2 consensus are highlighted in yellow. Potential phosphorylation sites near the PTS2 were predicted using the Netphos 3.1 Server (http://www.cbs.dtu.dk) and are underlined.

However, *Pp*MdhA and *Pp*GpdA have a high probability of being targeted to the mitochondria and contain an identifiable mitochondrial presequence at the N-terminus based on the MitoProtII program (Claros & Vincens, 1996). More specifically, *Pp*MdhA has a probability of 0.948 and an 18 amino acid mitochondrial presequence (MLSTIAKRQFSSSASTA), while *Pp*GpdA has a probability of 0.6471 for being translocated to the mitochondria and a 24 amino acid mitochondrial presequence (MYLTSTVRALPVHFFRSRHCIRT) (Table 1). A probability

greater than 0.5 is more likely to be a mitochondrial protein (Claros & Vincens, 1996). *Sc*Mdh1 and *Sc*Gpd2 have a probability greater than 0.9 and are known to have a mitochondrial localization, which is similar to *Pp*MdhA that also has a high probability for mitochondrial targeting. *Pp*GpdA has a lower probability than the *S. cerevisiae* mitochondrial NADH shuttling proteins (Mdh1 and Gpd2), but a higher probability than cytosolic or peroxisomal shuttling dehydrogenases (*Sc*Mdh2, *Sc*Mdh3, and *Sc*Gpd1). In conclusion, *Pp*MdhA has a high chance of being a mitochondrial enzyme and could be the homolog of *Sc*Mdh1. *Pp*MdhB does not have a distinct targeting signal, so the putative localization cannot be elucidated *in silico* and similarly with *Pp*GpdA, the localization is not evident, but it has a low probability of being a mitochondrial enzyme.

Table 1. *In silico* analysis of malate and glycerol 3-phosphate dehydrogenases in *P. pastoris* and *S. cerevisiae*. PTS1 scores were based on the C-terminal sequences of the dehydrogenases. Scores greater than 0 typically have a predictable PTS1. MitoProt scores were based on the N-terminal predictions for mitochondrial presequences. MitoProtII scores with a probability greater than 0.5 are more likely to be mitochondrial proteins.

Protein	C-terminal	PTS1 Score	N-terminal	MitoProt Score
*Sc*Mdh1	NIEKGVNFVASK	-48.5	MLSRVAKRAFSSTVANP	0.9910
*Sc*Mdh2	GLEFVASRSASS	-38.2	Not predictable	0.0376
*Sc*Mdh3	KGKSFILDSSKL	4.9	Not predictable	0.1859
*Pp*MdhA	IAKGQEFVKQNP	-37.7	MLSTIAKRQFSSSASTA	0.9549
*Pp*MdhB	NIAKGTAFIAGN	-52.6	Not predictable	0.1410
*Sc*Gpd1	PDMIEELDLHED	-101.6	MSAAADRLNLTSGHLNAGRKRS	0.3132
*Sc*Gpd2	PEMIEELDIDDE	-86.8	MLAVRRLTRYTFLKRTH	0.9932
*Pp*GpdA	FNKTEDVKHWED	-58.1	MYLTSTVRALPVHFFRSRHCIRT	0.6471

2) Peroxisome biogenesis phenotype of NADH shuttling proteins

We have found that a functional OXPHOS is essential for peroxisome biogenesis and OXPHOS mutants such as the deletion of the *NDUFA9* gene resulted in no peroxisome

proliferation (Figure 6A). Ndufa9 (NADH dehydrogenase (ubiquinone) 1 alpha subcomplex, subunit 9) is an accessory component of complex I that accepts the electrons from NADH and transfers them to ubiquinone, a lipid soluble molecule, that carries the electrons from NADH through the mitochondrial membrane to the rest of the respiratory chain. In mammalian cells, NDUFA9 is important for complex I assembly (Baertling et al., 2017). In yeast, β-oxidation occurs exclusively at the peroxisome and during growth in oleate as the only carbon source, peroxisomes will produce NADH and acetyl-CoA, which will need to shuttle to the mitochondria for energy production (ATP) and carbon assimilation.

To determine if NADH shuttling in *P. pastoris* affects peroxisome proliferation as found in the OXPHOS mutants, we generated individual and double mutants of the NADH shuttle proteins and observed the effect on peroxisome proliferation in oleate medium using Pex3-GFP and BFP-SKL as peroxisome markers. Pex3-GFP is a peroxisomal membrane protein with GFP fused to the C-terminus and BFP-SKL has a PTS1 fused to the C-terminus of BFP in order to check if peroxisomes are import competent. Compared to the wildtype, Δ*gpdA* displayed normal peroxisome proliferation in oleate, while the individual mutants Δ*mdhA* and Δ*mdhB* showed reduced peroxisome proliferation in oleate medium (Figure 6B). Similarly to *S. cerevisiae*, the double mutants Δ*mdhA* Δ*gpdA* and Δ*mdhB* Δ*gpdA* showed weak or no peroxisome proliferation, a phenotype which resembled the OXPHOS mutants (Figure 6C), suggesting that MdhA-B and GpdA may be playing a shuttling role for re-oxidizing NADH produced in the peroxisomes from fatty acid β-oxidation.

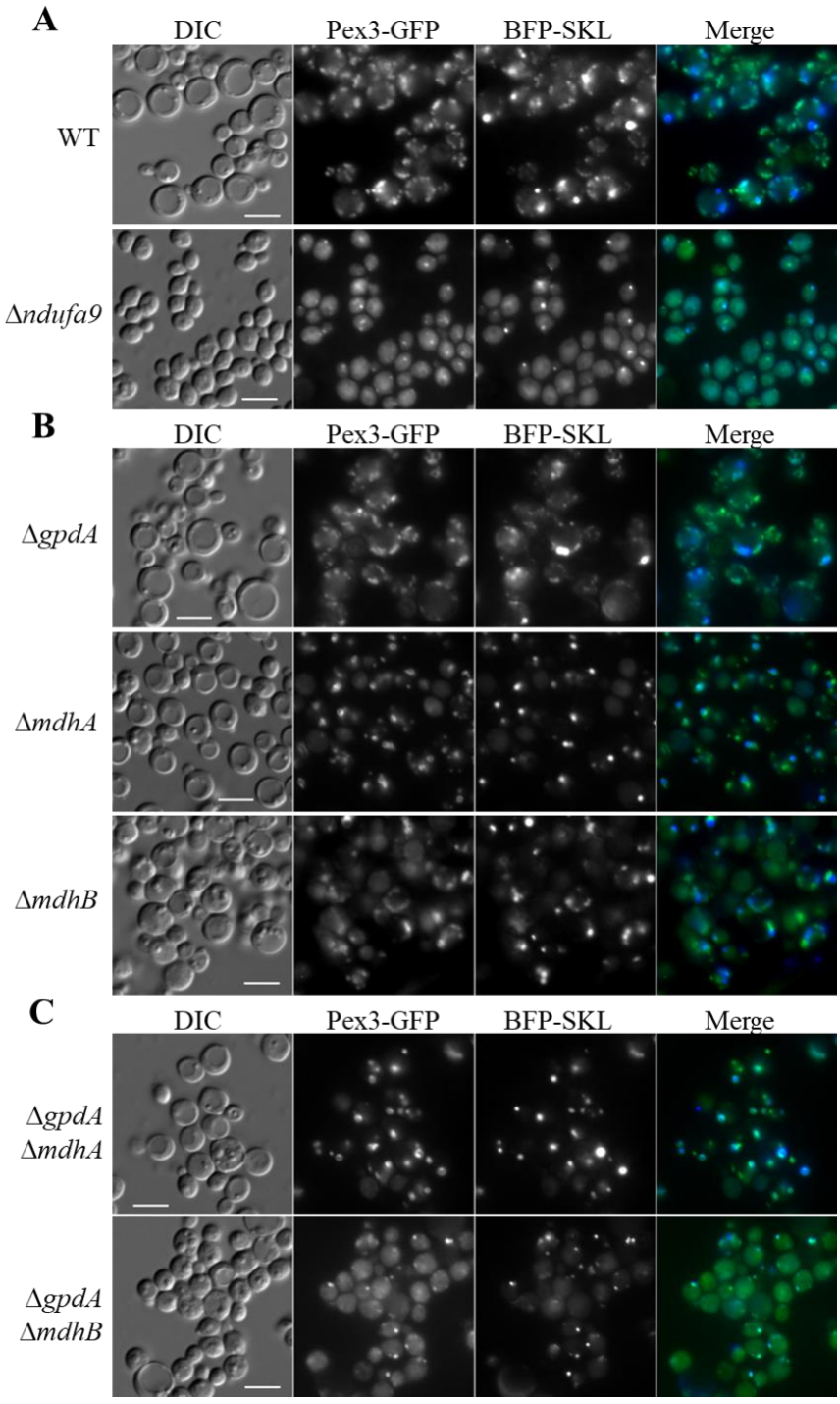

Figure 6. Peroxisome proliferation defect of Δ*ndufa9* cells and NADH shuttling dehydrogenase mutants in *P. pastoris*. Fluorescence microscopy of several strains grown in oleate for 24 hours. **A)** Wild-type cells and mutant of the accessory subunit of complex I, Ndufa9. **B)** Malate dehydrogenase A and B, and glycerol 3-phosphate dehydrogenase A mutant strains **C)** Double mutants of GpdA and MdhA/B. Peroxisomes were visualized using a peroxisomal membrane protein (Pex3-GFP) and peroxisomal matrix protein (BFP-SKL). Bars: 5μm.

4) Localization of *Pp*MdhA-GFP, *Pp*MdhB-GFP and *Pp*GpdA-GFP in different carbon sources

We found *Pp*MdhA and *Pp*GpdA, both lacking an identifiable PTS1 sequence at the C-terminus and PTS2 sequence at the N-terminus, to have a high likelihood of mitochondrial targeting *in silico*. Of the three dehydrogenases, *Pp*MdhB has the lowest probability for mitochondrial targeting, hence the best candidate to be at least partially localized at the peroxisome. In *S. cerevisiae*, Mdh3 is important for intraperoxisomal redox balance of NAD(H) in oleate, but not in other media. If *P. pastoris* shares a similar shuttling mechanism with *S. cerevesiae* for transporting NADH from the peroxisome to the mitochondria and maintaining the intraperoxisomal redox balance in oleate, then it would be important to study the localization of *Pp*MdhA, *Pp*MdhB, and *Pp*GpdA in glucose, methanol, and oleate.

To localize the NADH shuttling proteins in *P. pastoris*, we fused GFP to the C-terminus of *Pp*MDHA/B and *Pp*GPDA, as there was no obvious SKL, which could be masked by a C-terminus fusion, and expressed these GFP fusion proteins from their endogenous promoters in wild-type cells. We also transformed a mitochondrial and peroxisomal marker, Tom20-mRFP and BFP-SKL, respectively, into the wild-type strains containing the shuttling dehydrogenase-GFP fusion proteins to determine if there was localization at the mitochondria or peroxisome. Although *Pp*GpdA has a lower chance for mitochondrial targeting than *Pp*MdhA, both *Pp*MdhA-GFP and *Pp*GpdA-GFP appeared to not only have partially cytosolic fluorescence, but also colocalization with the mitochondrial marker in glucose, methanol, and oleate media, suggesting that these two proteins may possess dual localization in *P. pastoris* in all three media (Figure 7A and 7B).

In contrast, *Pp*MdhB-GFP differed in that it appeared cytosolic in all three media with no obvious intra-organelle localization (Figure 7C). Based on the cytosolic and mitochondrial

localization, supported by the likelihood for mitochondrial targeting, *Pp*GpdA could be the homolog of *Sc*Gpd2. The mitochondrial localization confirmed the high probability for mitochondrial targeting for *Pp*MdhA making it likely that this is the homolog of *Sc*Mdh1. Finally, based on the cytosolic localization, *Pp*MdhB is like *Sc*Mdh2.

Based on the NADH shuttling proteins localization in all the media tested in *P. pastoris*, it would appear that NADH should not shuttle out of the peroxisome, as neither *Pp*Mdh isoforms nor *Pp*Gpd have a peroxisomal localization. However, the peroxisome-deficient phenotype observed in peroxisome proliferation conditions caused by single and double mutants of the NADH shuttling proteins, indicated otherwise, which would need to be further investigated.

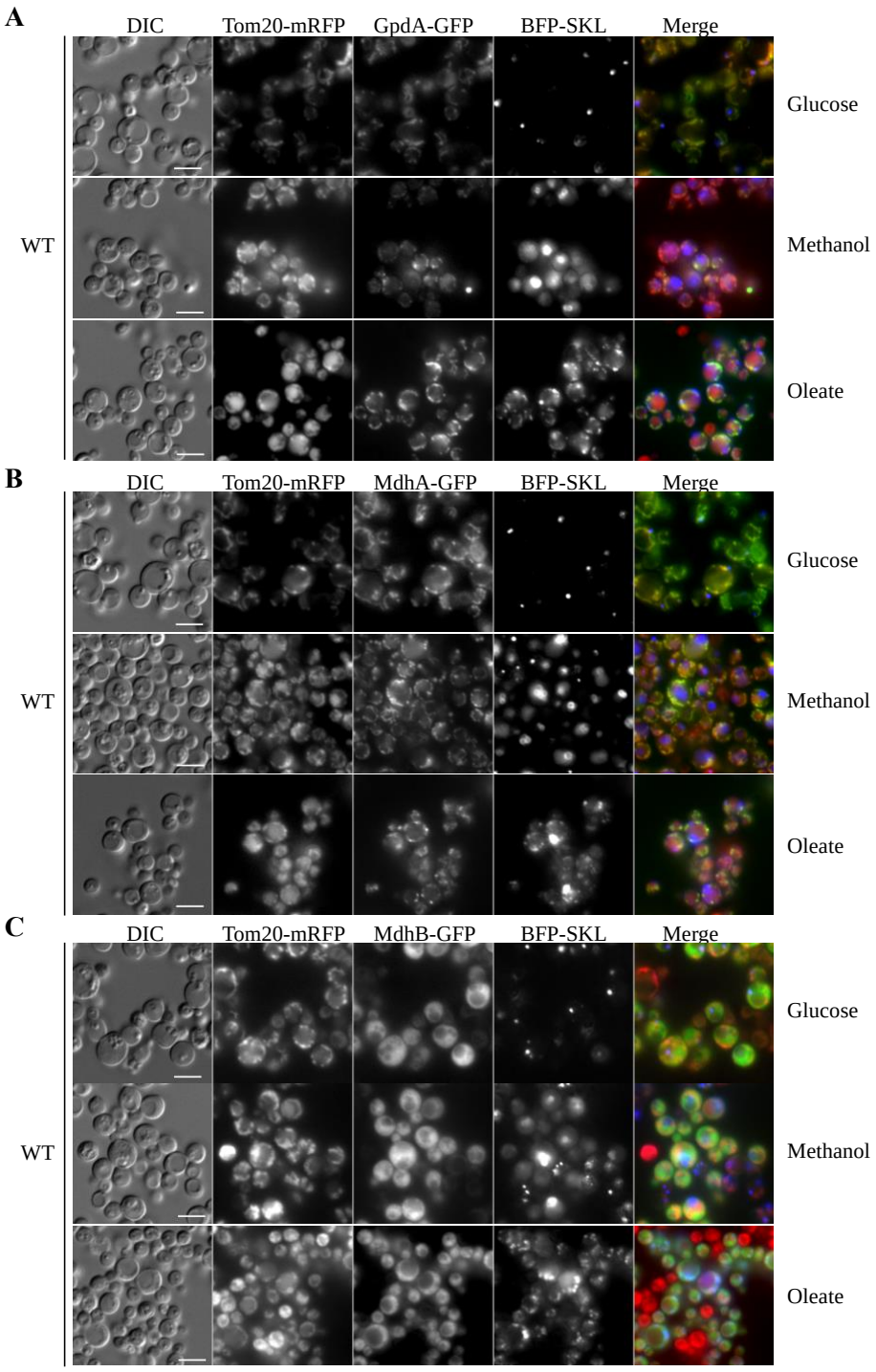

Figure 7. Localization of NADH shuttling proteins fused with GFP. Fluorescence microscopy of strains grown in glucose, methanol, and oleate overnight. GFP was fused to the C-terminus of the NADH shuttling proteins and the fusion proteins were expressed from their endogenous promoters. **A)** Wild-type cells expressing GpdA-GFP **B)** Wild-type cells expressing MdhA-GFP **C)** Wild-type cells expressing MdhB-GFP. Colocalization studies with the mitochondria and peroxisome was observed with Tom20-mRFP and BFP-SKL as the mitochondrial peroxisomal markers, respectively. Bars: 5μm.

5) Developing an assay to improve detection of peroxisomal localized proteins

We hypothesized that a small fraction of the NADH shuttling proteins could localize at the peroxisome and it was probably drowned out by the predominantly cytosolic fraction. To be able to detect a putative small peroxisomal fraction, we used a technique called bimolecular fluorescence complementation (BiFC). BiFC uses a fluorescent Venus protein that is split into two, non-fluorescent halves called VN and VC. VN and VC are typically fused to two proteins that may physically interact or be in close proximity to bring VN and VC together to reconstitute GFP and yield fluorescence (Shyu et al., 2008). For investigating the localization of the NADH shuttling proteins, we took advantage of the latter case. With this purpose in mind, we chose to target the VN moiety to the peroxisome through the most efficient PTS1 pathway, by fusing the PTS1 (SKL) at the C-terminus of VN and fusing the NADH shuttling proteins with VC. To increase the chances that VN and VC find each other and yield fluorescence, we decided to overexpress both fusion proteins. The PTS1 pathway is extremely efficient and a large fraction of VN-SKL was expected to localize to the peroxisomes (DeLoache et al., 2016). If a small fraction of the NADH shuttling proteins fused to VC is imported to the peroxisome, the fluorescence at the peroxisome should exceed the fluorescence at the cytosol, allowing detection by regular fluorescence microscopy (Figure 8).

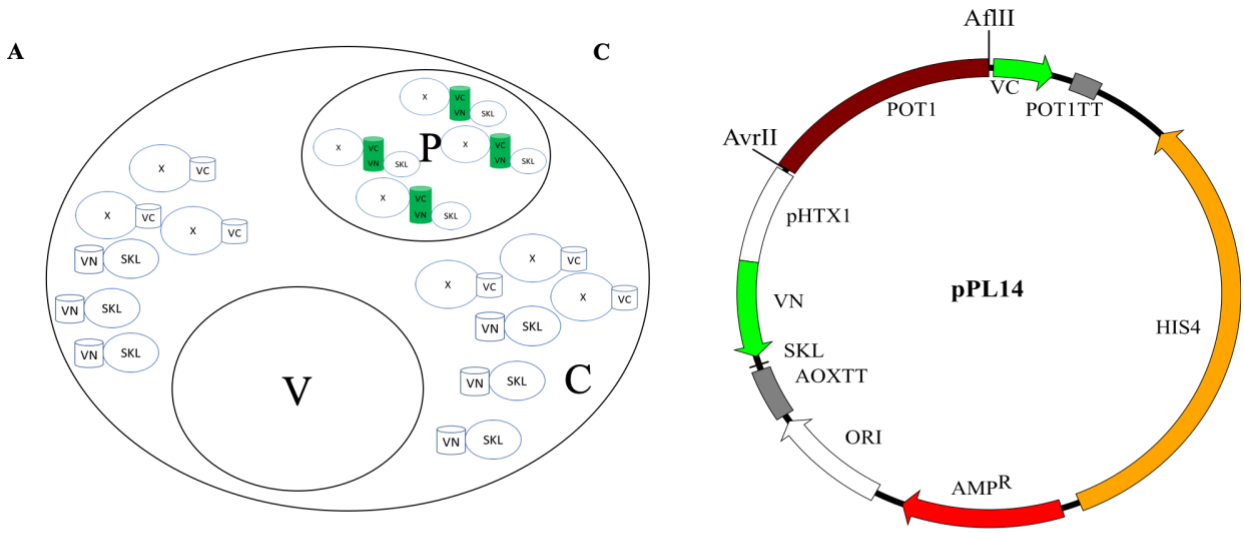

B

Protein of Interest-VC	VN-SKL	Fluorescence in Peroxisomes
Cytosol	Peroxisome	No
Peroxisome	Peroxisome	Yes
Mitochondria	Peroxisome	No
Cytosol & Peroxisome	Peroxisome	Yes
Cytosol & Mitochondria	Peroxisome	No
Cytosol, Peroxisome, & Mitochondria	Peroxisome	Yes

Figure 8. Expected fluorescence using the divergent BiFC assay. A) Schematic representation of the expected outcome of the assay (P-peroxisome, C-cytosol, V-vacuole). **B)** Potential subcellular localizations that may yield peroxisomal fluorescence. **C)** Plasmid construct (TT-terminator, *HIS4*- histidine selection marker for yeast, Amp$_R$- ampicillin resistance gene, pHTX1- strong constitutive bidirectional promoter). AvrII and AflII were used for double digestion to replace Pot1 with our protein of interest.

5A) The positive control

To prove the concept of the divergent BiFC assay, we co-expressed together with VN-SKL, a peroxisomal non-interacting protein, thiolase, fused with VC at its C-terminus. Thiolase (Pot1) is an enzyme synthesized in the cytosol and imported through the PTS2 pathway into the peroxisome where it catalyzes the last step of the β-oxidation pathway (Elgersma et al., 1998). Since the PTS2 nonapeptide is at the amino terminus of Pot1, the VC moiety was fused at the C-terminus. This way, both the PST2-containing protein and PTS1 fused at the C-terminus of VN can still be recognized by their respective PTS receptors for import into the peroxisome. The overexpression of these non-interacting proteins containing a PTS would increase the amount of

Pot1 and SKL at the peroxisome, a confined compartment, crowding together VN and VC to yield fluorescence. For simplicity, both Pot1-VC and VN-SKL were expressed from a bidirectional, constitutively-active *HTX1* promoter in a single plasmid construct that also served as a background plasmid for future experiments by simply swapping out Pot1 with another protein of interest (Figure 8).

The plasmid, co-expressing Pot1-VC and VN-SKL, was transformed and integrated into the genome of *P. pastoris* wild-type cells expressing Pex3-mRFP from its own promoter as a peroxisomal marker and analyzed by fluorescence microscopy after induction in glucose, methanol, and oleate medium (Figure 9). *P. pastoris* glucose-grown cells contain a single small peroxisome (area: ~0.05 μm^2) and when cells are grown in media requiring peroxisome metabolism, the peroxisome size and number increase (Nazarko et al., 2009). The most commonly used media for peroxisome proliferation in *P. pastoris* are oleate and methanol. When cells are grown in oleate media overnight, peroxisome number and area increase to ~6 and to ~0.08 μm^2, respectively, and peroxisomes are dispersed in the cytosol near the cell periphery. Similarly, when cells are grown in methanol media overnight, peroxisome number and area increase to ~4 and to ~0.4 μm^2, respectively, and are clustered.

As hypothesized, the overexpression of the two peroxisomal chimera proteins Pot1-VC and VN-SKL, showed a strong fluorescence at the peroxisome in every media confirmed by the colocalization with Pex3-mRFP, indicating the two non-fluorescent halves of the Venus proteins were reconstituted at the peroxisomes, most likely due to their proximity created by their high abundance in a confined area (Figure 9).

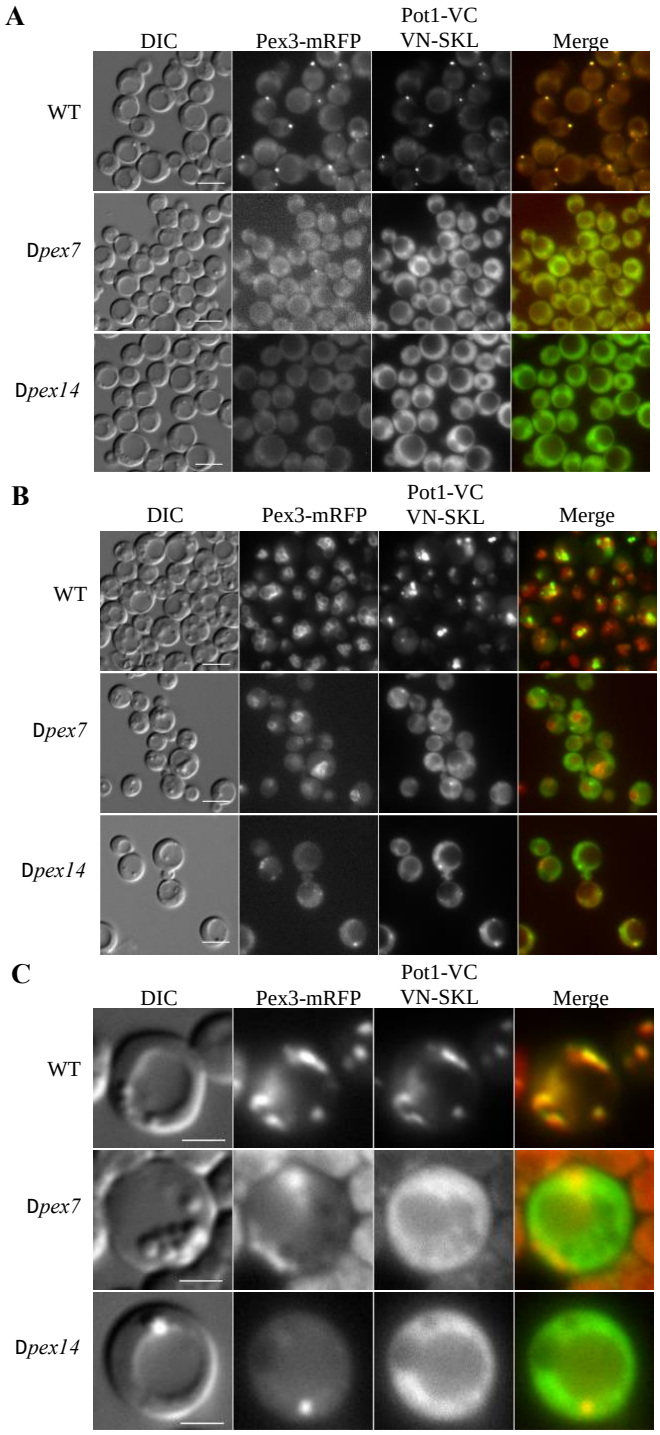

Figure 9. Confirming the feasibility of the divergent BiFC assay using known peroxisomal matrix proteins. The PTS2-containing protein, thiolase, was fused to VC (Pot1-VC) and the PTS1 was fused to VN (VN-SKL). **A)** Strains were grown in glucose overnight. Bars: 5µm. **B)** Strains were grown in methanol overnight. Bars: 5µm. **C)** Strains were grown in oleate overnight. Bars: 2µm. Peroxisome were visualized using Pex3-mRFP.

5B) The negative controls

To confirm that the peroxisomal fluorescence observed in our divergent BiFC assay was a consequence of the Venus reconstitution in the peroxisomal matrix and not a weak fluorescence of the Venus moiety itself, we knocked out different essential components of peroxisomal matrix protein import. With this purpose, we transformed the plasmid co-expressing Pot1-VC and VN-SKL into cells mutated for the PTS2 receptor (Δ*pex7*) and for the peroxisomal receptor docking protein (Δ*pex14*) and tested them in glucose, methanol, and oleate (Figure 9). We also transformed Pex3-mRFP, a peroxisomal membrane protein, into the *pex* mutant strains as a peroxisome marker.

When we analyzed cells lacking the PTS2 receptor in the three media, no fluorescence was observed at the peroxisome, although we noticed some cytosolic fluorescence. These results were somehow expected at least for the lack of peroxisomal fluorescence, as Pot1 was not supposed to be imported into the peroxisome without its PTS2 receptor, while the cytosolic fluorescence was unexpected because VN-SKL was still supposed to be imported into the peroxisome in the presence of the PTS1 receptor, which might indicate a fair amount of the VN-SKL synthesized in the cytosol remained there. When we analyzed cells lacking the peroxisomal receptor docking protein Pex14, no peroxisomal fluorescence was observed in any media as expected, because neither the PTS1 receptor nor the PTS2 receptor could dock in the peroxisomal membrane to import their respective cargoes. Similar to the result in the Δ*pex7* cells, a cytosolic fluorescence was observed in the Δ*pex14* cells, although in this case the result was highly expected as both VN-SKL and Pot1-VC were not supposed to be imported. In addition, the fluorescence in the cytosol indicated the constitutive *HTX1* promoter is strong enough to crowd even the cytosol with the two Venus moieties.

To verify the specificity of the divergent BiFC assay, we replaced the peroxisomal *POT1* by glyceraldehyde-3-phosphate dehydrogenase (*GAPDH*) that is involved in glycolysis and gluconeogenesis and localized exclusively in the cytoplasm and cell wall. We co-expressed GAPDH-VC and VN-SKL in wild-type cells and observed the fluorescence in glucose, methanol, and oleate. In all three media, the fluorescence was localized in the cytosol and no colocalization with Pex3-mRFP was observed, similar to Pot1 in Δ*pex7* and Δ*pex14* (Figure 10).

Thus, we demonstrated that the divergent BiFC assay worked as expected with a strong peroxisomal fluorescence for Pot1, which could be abolished by the deletion of *PEX7* and *PEX14* genes, and similarly no peroxisomal fluorescence was observed when we swapped Pot1 by the cytosolic protein Gapdh in wild-type cells.

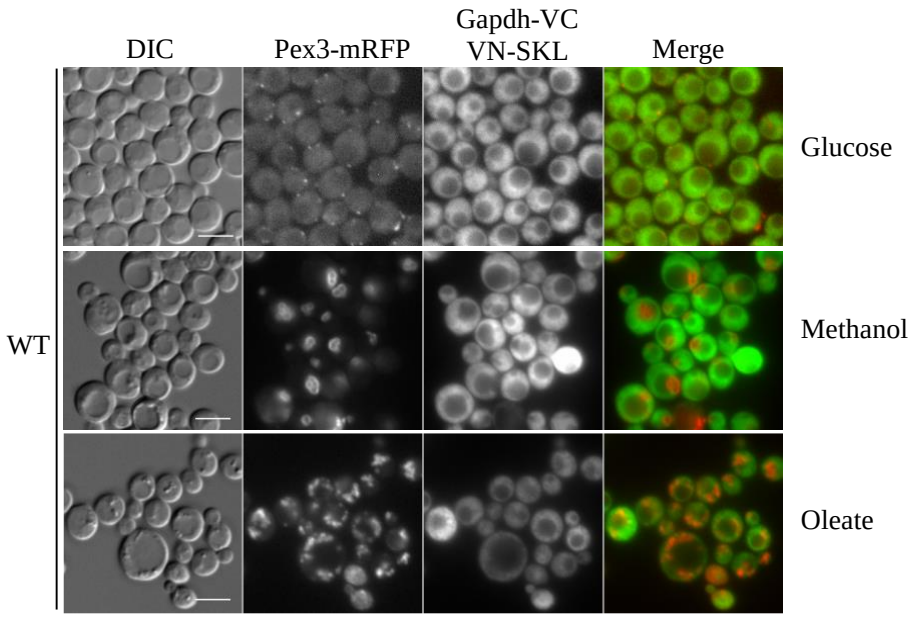

Figure 10. Peroxisomal fluorescence is not observed for a cytosolic protein (Gapdh) using the divergent BiFC assay. Strains were grown in glucose, methanol, and oleate overnight. Peroxisomes were visualized using Pex3-mRFP and the peroxisomal matrix protein, VN-SKL. Bars: 5μm.

5C) Testing the localization of the NADH shuttling proteins using the divergent BiFC assay

Given the detection of peroxisomal fluorescence and specificity using the divergent BiFC assay in our controls, we then used this approach to test the localization of our NADH shuttling

proteins by transforming *Pp*GpdA-, *Pp*MdhA-, or *Pp*MdhB-VC and VN-SKL plasmids into wild-type cells. The Pot1-VC plasmid served as a background plasmid as we swapped Pot1 for Mdh or Gpd, fusing VC to the C-terminus of the NADH shuttling proteins that do not possess a recognizable PTS1 and blocking peroxisomal import through the PTS1 pathway. We also transformed Pex3-mRFP, a peroxisomal membrane protein, into these strains to follow peroxisomes and determine if these shuttling proteins colocalize with peroxisomes. If peroxisomal fluorescence is observed, then it is possible that the proteins may be imported into the peroxisomal matrix through the PTS2 pathway, because the N-terminal PTS2 is not blocked by a VC tag and would still be recognized by the PTS2 receptor for peroxisomal import.

In wildtype, we observed mitochondrial fluorescence for *Pp*GpdA and *Pp*MdhA in glucose, methanol, and oleate (Figure 11 and 12). Peroxisomal fluorescence was not observed, suggesting no colocalization with Pex3-mRFP, as expected if VN-SKL was imported into the peroxisome and *Pp*GpdA or *Pp*MdhA was imported to the mitochondria. Based on our sequence analysis, we expected *Pp*GpdA and *Pp*MdhA to have a mitochondrial localization, but we did not expect to be able to detect mitochondrial fluorescence, unless VN-SKL, a peroxisomal matrix protein, was somehow mislocalized to the mitochondria. For the VN-SKL imported into the peroxisome and the *Pp*GpdA or *Pp*MdhA imported in the mitochondria, we would not expect to observe peroxisomal or mitochondrial fluorescence, or even Venus reconstitution in the peroxisome or mitochondria without both halves of the Venus protein present in either organelle. Although VN-SKL would be expected to localize at the peroxisome, it is possible that *Pp*GpdA or *Pp*MdhA in the cytosol reconstituted the Venus protein with a portion of VN-SKL synthesized in the cytosol due to protein overexpression by the *HTX1* promoter and the nature of BiFC, binding the two proteins irreversibly in the cytosol, and was ultimately targeted to the mitochondria despite

possessing targeting signals to two different organelles. An alternative explanation would be that due to the overexpression of *Pp*GpdA or *Pp*MdhA , a large fraction accumulated on the surface of the outer membrane of the mitochondria during the import and can still come in contact with VN-SKL in the cytosol, yielding fluorescence.

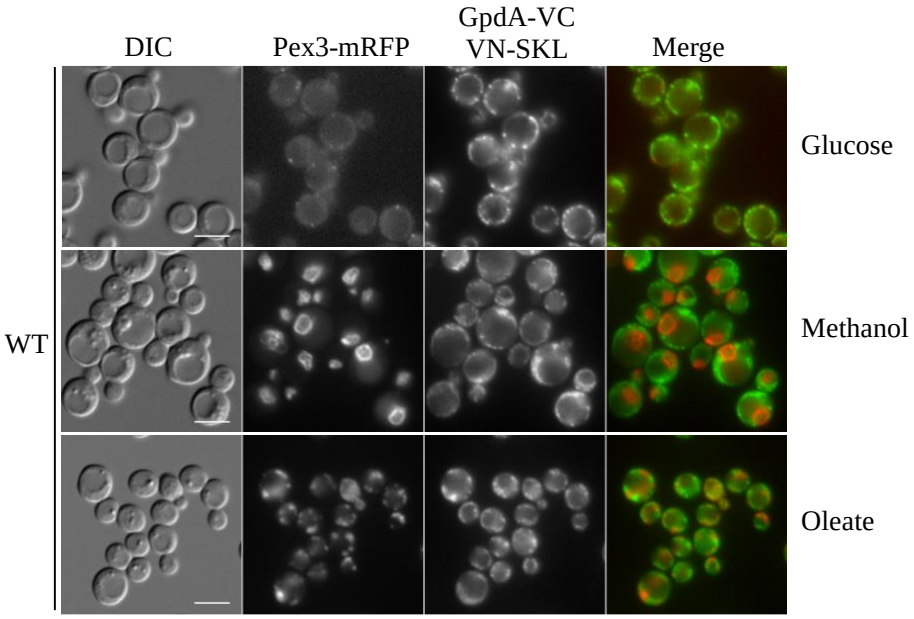

Figure 11. Localization of *Pp*GpdA in wild-type cells using the divergent BiFC assay. Strains were grown in glucose, methanol, and oleate overnight. Peroxisomes were visualized using Pex3-mRFP. Bars: 5µm.

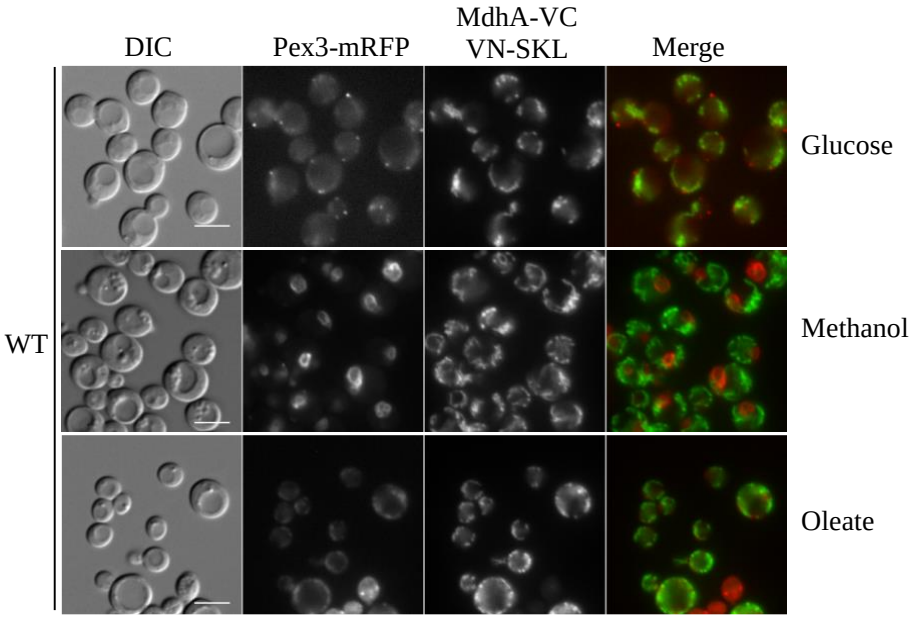

Figure 12. Localization of *Pp*MdhA in wild-type cells using the divergent BiFC assay. Strains were grown in glucose, methanol, and oleate overnight. Peroxisomes were visualized using Pex3-mRFP. Bars: 5µm

However, in wild-type cells, *Pp*MdhB displayed cytosolic fluorescence in glucose and methanol, but in oleate, *Pp*MdhB appeared partially peroxisomal and cytosolic (Figure 13A). Similar to Gapdh, *Pp*MdhB exhibited cytosolic fluorescence, as *Pp*MdhB remained mostly in the cytosol and reconstituted the Venus protein with a portion of VN-SKL synthesized in the cytosol, indicating that *Pp*MdhB is a cytosolic protein. In oleate, *Pp*MdhB displayed cytosolic and peroxisomal fluorescence that colocalized with Pex3-mRFP, suggesting that *Pp*MdhB has a dual localization to the cytosol and peroxisome in this medium. Along with VN-SKL, *Pp*MdhB was imported into the peroxisome, crowding and reconstituting the Venus protein in the peroxisome enough to yield peroxisomal fluorescence.

In order to further study peroxisomal import of *Pp*MdhB, we transformed *Pp*MdhB-VC and VN-SKL, as well as Pex3-mRFP, into Δ*pex7* and Δ*pex14*. In oleate, similar to Pot1 in Δ*pex7* and Δ*pex14*, *Pp*MdhB displayed cytosolic fluorescence in Δ*pex7*, suggesting import through the PTS2 pathway. As expected for peroxisomal import of *Pp*MdhB, no peroxisomal fluorescence was observed in Δ*pex14* cells. Cytosolic fluorescence of *Pp*MdhB in Δ*pex7* and Δ*pex14* indicated reconstitution of the VN moieties in the peroxisome (Figure 13B).

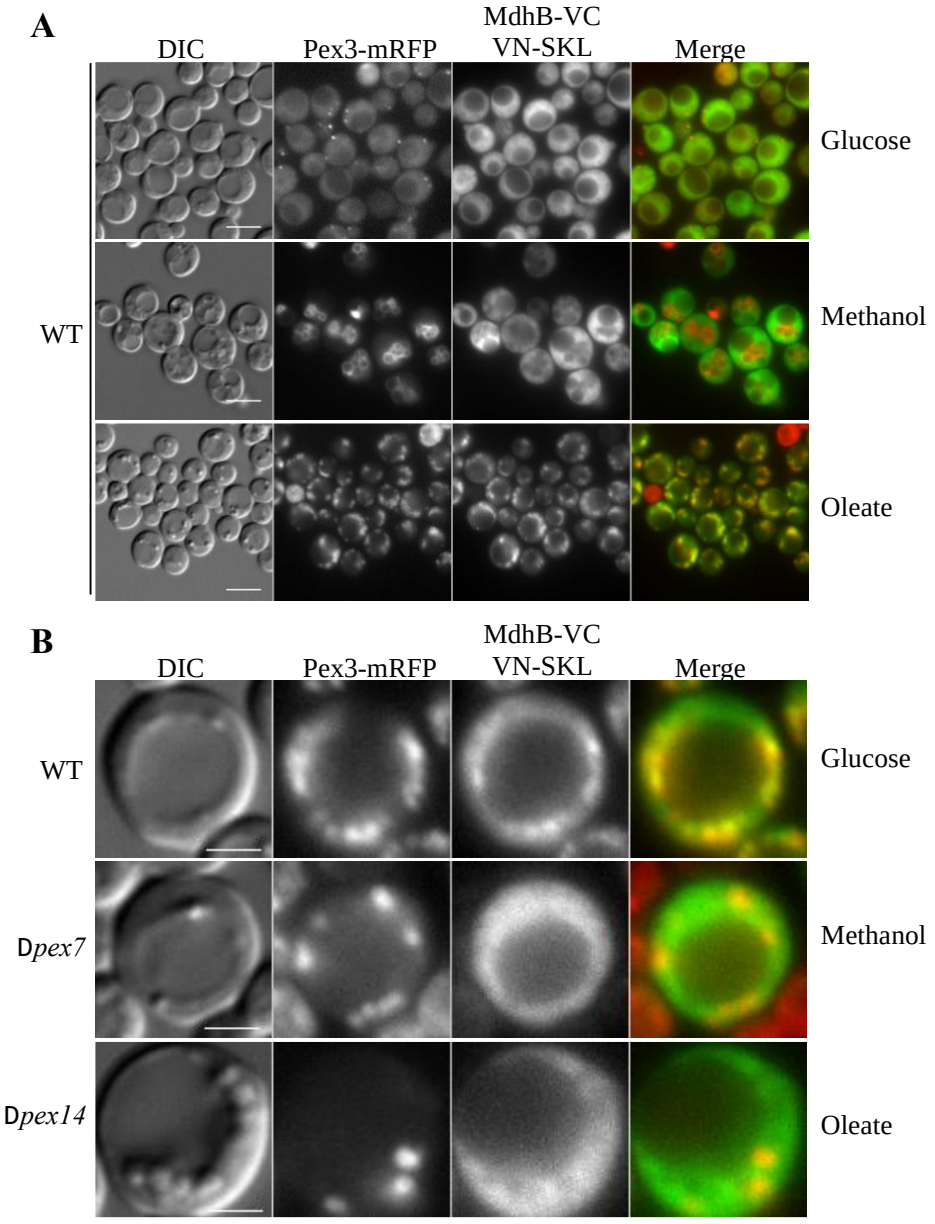

Figure 13. Localization of *Pp*MdhB using the divergent BiFC assay. A) Wild-type cells were grown in glucose, methanol, and oleate overnight. Bars: 5µm. **B)** Wild-type, Δ*pex7*, and Δ*pex14* cells grown in oleate overnight. Bars: 2µm. Peroxisomes were visualized using Pex3-mRFP.

We did not find any apparent PTS1 or PTS2 based on our sequence analysis, so it is possible that *Pp*MdhB may have a non-canonical PTS1 created from an unknown mechanism. For this reason, we also fused VC to the N-terminus of *Pp*MdhB (VC-*Pp*MdhB) and transformed VC-

*Pp*MdhB and VN-SKL into wild-type cells. Using the divergent BiFC assay, we found VC-*Pp*MdhB to be cytosolic in glucose, methanol, and oleate. In contrast to *Pp*MdhB-VC, VC-*Pp*MdhB has the N-terminus blocked preventing the PTS2 receptor from binding to a potential PTS2 at the N-terminus, and VC-*Pp*MdhB appeared fully cytosolic in oleate, suggesting that *Pp*MdhB may possess a PTS2 at the N-terminus, in support of the result of *Pp*MdhB-VC showing cytosolic fluorescence in Δ*pex7* (Figure 14). It is possible that placing a tag at the N-terminus may affect the protein folding and function of *Pp*MdhB.

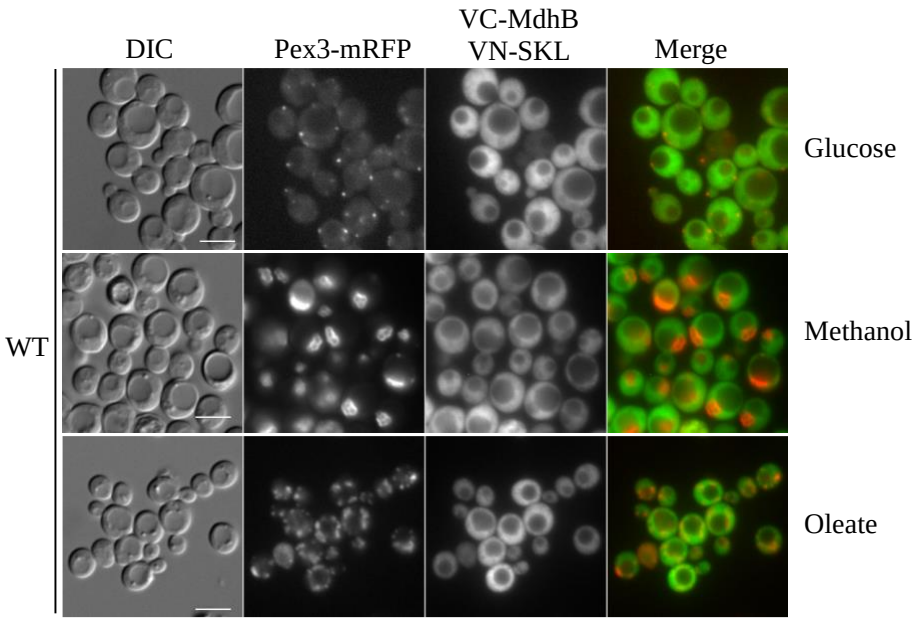

Figure 14. MdhB fused with VC at its N-terminus shows only cytosolic localization using the divergent BiFC assay. Strains were grown in glucose, methanol and oleate overnight. Peroxisomes were visualized using Pex3-mRFP. Bars: 5μm.

As an unintended consequence of the divergent BiFC assay, we detected mitochondrial fluorescence for *Pp*GpdA and *Pp*MdhA in every media, confirming the results for *Pp*MdhA-GFP and *Pp*GpdA-GFP. Using the divergent BiFC assay, the cytosolic fluorescence observed for *Pp*MdhB in wild-type cells in glucose and methanol was in agreement with our *Pp*MdhB-GFP results. However, we also discovered cytosolic and peroxisomal fluorescence, as well as colocalization with Pex3-mRFP, for *Pp*MdhB in oleate, suggesting dual localization depending on

the media. When we used Δ*pex7* and Δ*pex14* with *Pp*MdhB-VC, or fused VC to the N-terminus of *Pp*MdhB (VC-*Pp*MdhB), *Pp*MdhB was cytosolic in comparison to its location in the wild-type cells, suggesting import through the PTS2 pathway with a potential PTS2 at the N-terminus and reconstitution of the Venus protein in the peroxisome to yield peroxisomal fluorescence. Thus, the divergent BiFC assay revealed a peroxisomal fraction of *Pp*MdhB that may have been masked by the largely cytosolic isoform when *Pp*MdhB was expressed from its own promoter as opposed to a strong constitutive promoter.

6) Expressing MdhB-GFP from the *AOX* promoter to confirm peroxisomal localization

We wanted to confirm the peroxisomal fluorescence of *Pp*MdhB in oleate found in our divergent BiFC assay using our original strategy of fusing GFP to the C-terminus of *Pp*MdhB. Instead of expressing *Pp*MdhB from its own promoter that may produce an abundance of *Pp*MdhB masking the peroxisomal isoform with a large cytosolic presence, we expressed *Pp*MdhB-GFP from the alcohol oxidase promoter that is tightly regulated, in an effort to reduce the cytosolic fluorescence and to make the peroxisomal fluorescence more apparent. The *AOX* promoter is induced in the presence of methanol, strongly repressed by glucose, and not expressed in oleate. We transformed the plasmid containing *Pp*MdhB-GFP expressed from the *AOX* promoter into wild-type cells, as well as plasmids expressing Tom20-mRFP and BFP-SKL as mitochondrial and peroxisomal markers, respectively, for colocalizations studies.

As a control, we induced expression of *Pp*MdhB-GFP by adding methanol to the media and found that *Pp*MdhB-GFP was fully cytosolic when cells were grown in methanol overnight (Figure 15A). There was no colocalization with our peroxisomal and mitochondrial markers. To control the levels of *Pp*MdhB, we turned on expression of *Pp*MdhB and peroxisome proliferation

for only 2h in methanol, turned off *Pp*MdhB expression in glucose for 1h, and finally transferred the wild-type cells to oleate media for peroxisome proliferation overnight. Glucose should repress the *AOX* promoter and turn off peroxisome proliferation in methanol that usually results in clustered peroxisomes as observed in our control. With a limited production of *Pp*MdhB, we expected a portion of *Pp*MdhB would remain in the cytosol, while another portion would localize at the peroxisome in oleate. Using this approach, we were indeed able to detect the peroxisomal isoform of *Pp*MdhB colocalizing with BFP-SKL (Figure 15B).

Therefore, we demonstrated that the peroxisomal fluorescence of *Pp*MdhB, colocalizing with Pex3-mRFP, observed using the divergent BiFC assay could be reproduced by controlling *Pp*MdhB-GFP levels expressed from the alcohol oxidase promoter that resulted in peroxisomal *Pp*MdhB colocalizing with the peroxisome marker, BFP-SKL, in oleate medium.

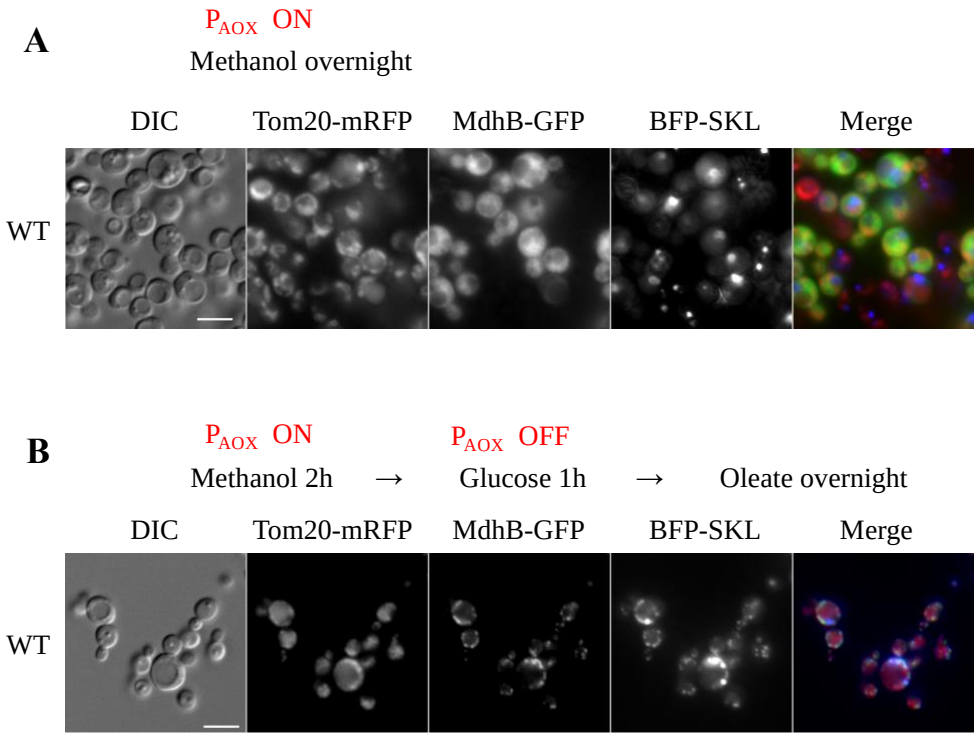

Figure 15. MdhB-GFP pulse-chase to observe small peroxisomal fraction. Fluorescence microscopy of MdhB-GFP expressed from the alcohol oxidase (*AOX*) promoter. **A)** Strains were grown on methanol overnight. **B)** Strains were grown on methanol for 2h to express MdhB-GFP from the *AOX* promoter (P_{AOX} ON), transferred to glucose for 1h to repress the *AOX* promoter (P_{AOX} OFF), and grown in oleate overnight to induce peroxisome proliferation. Colocalization studies with the mitochondria and the peroxisome were observed with Tom20-mRFP and BFP-SKL as the mitochondrial and peroxisomal markers, respectively. Bars: 5μm.

Discussion

Our lab found that mutants of complex I , where NADH feeds into the OXPHOS pathway, resulted in no peroxisome proliferation and this raised the question of whether the NADH shuttling proteins were implicated in peroxisome biogenesis. In *S. cerevisiae*, the NADH shuttling proteins have been well-studied and play a role in maintaining the intraperoxisomal redox balance in oleate medium. In contrast to *S. cerevisiae*, the NADH shuttling mechanism in *P. pastoris* has not been well-studied. Assuming that *P. pastoris* shares the same NADH shuttling mechanism as *S. cerevisiae*, we performed a protein BLAST to find and characterize the homologs of the NADH shuttling proteins. We generated single and double mutants that displayed reduced or no peroxisome proliferation, a shared phenotype with our complex I mutant. To characterize these NADH shuttling dehydrogenases implicated in peroxisome biogenesis, we performed an *in silico* analysis to predict the subcellular localization and then tested our predictions using fluorescence microscopy.

Based on our *in silico* analysis, we predicted that *Pp*GpdA and *Pp*MdhA are likely to localize at the mitochondria, while *Pp*MdhB is likely to be in the cytosol since it lacks obvious mitochondrial and peroxisomal targeting signals (Figure 4, 5 and Table 1). When we tagged the C-terminus of the NADH shuttling homologs with GFP and expressed them from their own promoters, we confirmed that *Pp*GpdA and *Pp*MdhA were indeed mitochondrial and *Pp*MdhB was cytosolic in glucose, methanol, and oleate media using fluorescence microscopy (Figure 7). However, the compromised peroxisome proliferation in Δ*mdhB* cells and the lack of proliferation in Δ*gpdA* Δ*mdhB* cells suggested that *Pp*GpdA and/or *Pp*MdhB could still localize at the peroxisome (Figure 6).

The divergent BiFC assay revealed a cytosolic and peroxisomal fluorescence of *Pp*MdhB in oleate medium using fluorescence microscopy and surprisingly, also confirmed the mitochondrial fluorescence of *Pp*GpdA and *Pp*MdhA in all three media, which was also found in the GFP fusion of our NADH shuttling proteins (Figure 11-13).

Both the GFP fusion of the NADH shuttling proteins and the divergent BiFC assay showed that MdhB was cytosolic in glucose and methanol, but differed in oleate with a cytosolic and peroxisomal localization using the divergent BiFC assay, as opposed to a fully cytosolic localization observed using the GFP fusion. To confirm the peroxisomal fluorescence of *Pp*MdhB found in our divergent BiFC assay, we returned to the original strategy of tagging MdhB with GFP, but instead of using the endogenous promoter, we expressed the protein from the inducible *AOX* promoter. Our pulse-chase assay confirmed that some MdhB is peroxisomal and supported our divergent BiFC assay results (Figure 15B).

Taken together, *Pp*GpdA may be the homolog of *Sc*Gpd2 based on its mitochondrial localization and may play a role in shuttling NADH from the cytosol to the mitochondria. In contrast to *S. cerevisiae*, *P. pastoris* does not appear to be shuttling NADH out of the peroxisome through the glycerol 3-phosphate shuttle, as peroxisomal fluorescence and colocalization with peroxisomal markers for *Pp*GpdA were not observed. *Pp*MdhA may be the homolog of *Sc*Mdh1 based on its mitochondrial localization and may play a role in the TCA cycle in the mitochondria, in addition to regenerating NADH in the mitochondria that was shuttled from the cytosol to the mitochondria through the malate shuttle. Overall, it appears that NADH may be shuttled from the cytosol to the mitochondria through the malate dehydrogenase shuttle and/or the glycerol-3 phosphate dehydrogenase shuttle in *P. pastoris* (Figure 16).

In addition to the two mitochondrial NADH shuttling homologs, based on its cytosolic localization in all three media, *Pp*MdhB may be the homolog of *Sc*Mdh2 by shuttling NADH generated in the cytosol from glucose and methanol metabolism and NADH generated from the peroxisome from oleate metabolism to the mitochondria and may play a role in gluconeogenesis and the glyoxylate cycle (Figure 16).

However, based on its peroxisomal localization in oleate, *Pp*MdhB may also be the homolog of *Sc*Mdh3 in playing a role in β-oxidation by re-oxidizing NADH generated from fatty acid β-oxidation back to NAD^+ to maintain the intraperoxisomal redox balance (Figure 16). In the absence of *Pp*MdhB, the disruption of the intraperoxisomal balance could help explain the reduced peroxisome proliferation.

Although the mechanism for the peroxisomal localization of *Pp*MdhB in oleate remains unknown, we can rationalize that *Pp*MdhB has been peroxisomal and cytosolic in oleate meeting the metabolic requirement where NADH is produced in the peroxisome and needs to be shuttled out of the peroxisome for energy production, whereas in methanol NADH is primarily produced in the cytosol and would not need to shuttle out NADH from the peroxisome (Figure 2, 3, and 16).

*Pp*MdhB has a dual localization to the cytosol and peroxisome depending on the media. Interestingly, no recognizable PTS1 or PTS2 was found in *Pp*MdhB, although the peroxisomal trafficking of *Pp*MdhB depends on the PTS2 receptor, Pex7 (Figure 13B).

The small fraction of peroxisomal *Pp*MdhB observed in oleate medium may be due to various mechanisms. Similar to *P. pastoris*, *Y. lipolytica* also has two *MDH* genes, *YlMDH1* producing a mitochondrial isoform with a strong mitochondrial prediction based on MitoProt II and *Yl*MDH2 encoding a varying ratio of cytosolic and peroxisomal isoforms due to alternative splicing depending on the media (Kabran et al., 2012). Another possibility for creating two

isoforms of *Pp*MdhB is due to alternative start sites of transcription, such as in carnitine acetyltransferase (YCAT) in *S. cerevisiae* that is PTS1-dependent, in which a mitochondrial or peroxisomal isoform was made depending on the AUG site used for protein translation. Based on a 5' mRNA analysis, shorter transcripts that lacked the mitochondrial localization signal were created in oleate compared to glycerol and acetate conditions (Elgersma et al., 1995). In addition to alternative splicing and alternative transcription start sites, efficient ribosomal readthrough of malate dehydrogenase could create a PTS signal for peroxisomal localization. However, the stop codon for *Pp*MdhB is UAA, which has the least efficient readthrough, so this mechanism is not that likely. Finally, it is also possible that *Pp*MdhB could be entering the peroxisome by piggyback import, similar to *Sc*Pnc1 piggybacking onto *Sc*Gpd1, a PTS2-containing protein (Kumar et al., 2016).

To further elucidate the mechanism of import of *Pp*MdhB, we could use a yeast two-hybrid or co-immunoprecipitation approach to investigate the *Pp*MdhB interaction with Pex7 or peroxisomal matrix proteins. All of these tools are available in the lab, such as yeast two-hybrid constructs and libraries, as well as the antibodies for most of the PMPs and peroxisomal matrix proteins. Mainly, we could expect one of two outcomes: 1) a direct interaction with the Pex7 receptor, which indicates *Pp*MdhB might have a non-consensus PTS2 and we could try to map the region, or 2) a lack of interaction with the receptor and/or a direct interaction with a peroxisomal matrix protein, indicating a piggyback mechanism. In both cases, we expect some regulation mechanism to induce the translocation exclusively in oleate, that could be achieved by a modification around the non-consensus PTS2 or by piggyback import into a protein expressed only in oleate medium. All of these questions will be addressed in the future.

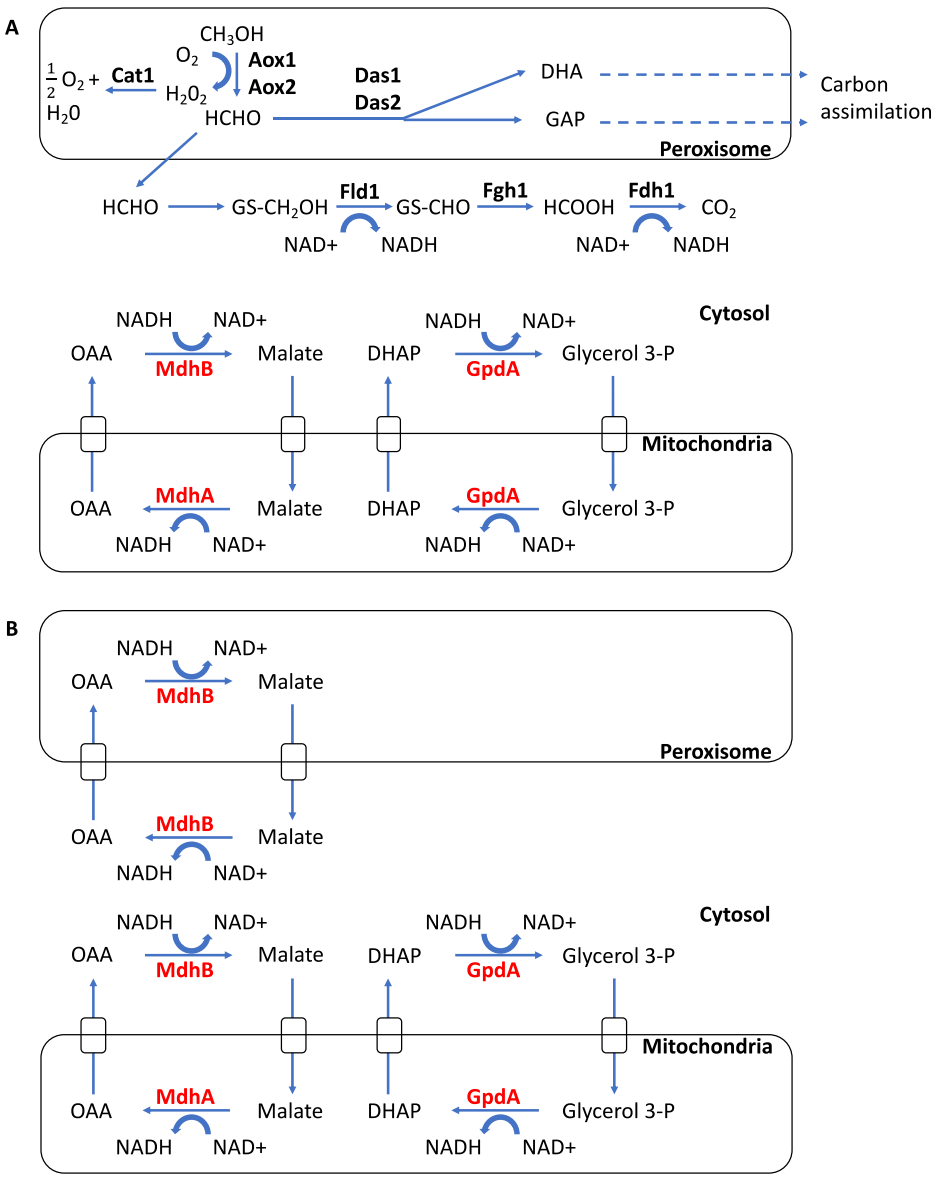

Figure 16. Proposed NADH Shuttling in *P. pastoris*. A) NADH shuttling in methanol. During methanol metabolism, methanol (CH_3OH) is broken down into formaldehyde (HCHO) producing hydrogen peroxide(H_2O_2) as a byproduct. Catalase (Cat1) converts hydrogen peroxide into water and oxygen. Some formaldehyde is converted in peroxisomes into DHA and GAP by Das1 and Das2 for carbon assimilation. Some formaldehyde also diffuses into the cytosol producing NADH through reactions involving Fld1 (formaldehyde dehydrogenase) and Fdh1 (formate dehydrogenase). NADH produced in the cytosol from methanol metabolism may be shuttled to the mitochondria for energy production through the malate or glycerol 3-phosphate (glycerol 3-P) shuttles. MdhB can convert oxaloacetate into malate oxidizing NADH into NAD+. Malate enters the mitochondria through a transporter. MdhA converts malate back to oxaloacetate reducing NAD+ to NADH. GpdA can convert dihydroxyacetone phosphate (DHAP) into Glycerol 3-P oxidizing NADH into NAD+. Glycerol 3-P can shuttle into the mitochondria where GpdA can regenerate NADH. **B)** NADH shuttling in oleate. NADH produced in the peroxisomes during oleate metabolism is shuttled out of the peroxisomes through the malate shuttle. MdhB converts oxaloacetate into malate, regenerating NAD+. MdhB regenerates NADH in the cytosol and also shuttles NADH from the cytosol to the mitochondria. MdhB re-oxidizes NADH back to NAD+, reducing oxaloacetate to malate , which is transported into the mitochondria, where MdhA regenerates NADH in the mitochondria, converting malate back to oxaloacetate. The glycerol 3-P shuttle can also shuttle NADH from the cytosol to the mitochondria.

Materials and Methods

Table 2. Yeast strains and plasmids

Yeast Strains	*Description*	*Source*
GS115	*his4 arg4*	Lab stock
PPY12h	*his4 arg4*	Lab stock
SEW1	Δ*pex3*::*ARG4 his4*	Lab stock
Δpex7	Δ*pex7*::*ARG4 his4*	Lab stock
JC404	Δ*pex14*::*ARG4 his4*	Lab stock
sPL66	GS115 + pJCF235-Zeo (P$_{PEX3}$-*PEX3-mRFP*)::*HIS4*(Zeocin^R) + pPL21 (P$_{HTX1}$-*GAPDH-VC* + *VN-SKL*)::*HIS4*	This study
sPL67	GS115 + pJCF235-Zeo (P$_{PEX3}$-*PEX3-mRFP*)::*HIS4*(Zeocin^R) + pPL14 (P$_{HTX1}$-*POT1-VC* + *VN-SKL*)::*HIS4*	This study
sPL68	GS115 + pJCF235-Zeo (P$_{PEX3}$-*PEX3-mRFP*)::*HIS4*(Zeocin^R) + pPL18 (P$_{HTX1}$-*MDHA-VC* + *VN-SKL*)::*HIS4*	This study
sPL69	GS115 + pJCF235-Zeo (P$_{PEX3}$-*PEX3-mRFP*)::*HIS4*(Zeocin^R) + pPL19 (P$_{HTX1}$-*MDHB-VC* + *VN-SKL*)::*HIS4*	This study
sPL70	GS115 + pJCF235-Zeo (P$_{PEX3}$-*PEX3-mRFP*)::*HIS4*(Zeocin^R) + pPL20 (P$_{HTX1}$-*GPDA-VC* + *VN-SKL*)::*HIS4*	This study
sPL75	Δpex7 + pJCF235-Zeo (P$_{PEX3}$-*PEX3-mRFP*)::*HIS4*(Zeocin^R) + pPL14 (P$_{HTX1}$-*POT1-VC* + *VN-SKL*)::*HIS4*	This study
sPL77	Δpex7 + pJCF235-Zeo (P$_{PEX3}$-*PEX3-mRFP*)::*HIS4*(Zeocin^R) + pPL19 (P$_{HTX1}$-*MDHB-VC* + *VN-SKL*)::*HIS4*	This study
sPL79	JC404 + pJCF235-Zeo (P$_{PEX3}$-*PEX3-mRFP*)::*HIS4*(Zeocin^R) + pPL14 (P$_{HTX1}$-*POT1-VC* + *VN-SKL*)::*HIS4*	This study
sPL81	JC404 + pJCF235-Zeo (P$_{PEX3}$-*PEX3-mRFP*)::*HIS4*(Zeocin^R) + pPL19 (P$_{HTX1}$-*MDHB-VC* + *VN-SKL*)::*HIS4*	This study
sPL93	GS115 + pJCF235-Zeo (P$_{PEX3}$-*PEX3-mRFP*)::*HIS4*(Zeocin^R) + pPL23 (P$_{HTX1}$-*VC-MDHB* + *VN-SKL*)::*HIS4*	This study
sJCF2177	SEW1 + pJCF533(P$_{PEX3}$-*PEX3-GFP*)::*HIS4* + pJCF742::P$_{GAPDH}$-*BFP-SKL*(Zeocin^R)	Lab stock
sJCF2649	sJCF2177 + Δ*GPDA*::*NAT*	Lab stock
sJCF2650	sJCF2177 + Δ*MDHA*::*HYGRO*	This study
sJCF2651	sJCF2177 + Δ*MDHB*::*HYGRO*	This study
sJCF2652	sJCF2177 + Δ*GPDA*::*NAT* + Δ*MDHA*::*HYGRO*	This study
sJCF2653	sJCF2177 + Δ*GPDA*::*NAT* + Δ*MDHB*::*HYGRO*	This study
sJCF2597	sJCF2177 + Δ*ndufa9::NAT*	This study
sJCF2169	PPY12h + pJCF523(P$_{TOM20}$-*TOM20-2xmCherry*)*::ARG4*(Hygro^R) pJCF402 *(*P$_{GAPDH}$-*BFP-SKL*)*::ARG4 his4*	This study
sJCF2771	sJCF2169 + pPL26(P$_{AOX1}$-*MDHB-GFP*)*::HIS4*	This study
sJCF2683	sJCF2169 + P$_{GPDA}$-*GPDA-GFP::HIS4*	This study
sJCF2682	sJCF2169 + P$_{MDHA}$-*MDHA-GFP::HIS4*	This study
sJCF2770	sJCF2169 + P$_{MDHB}$-*MDHB-GFP::HIS4*	This study

Table 2. Yeast strains and plasmids, continued

Plasmid	*Description*	*Source*
pPL14	P_{HTX1}-*POT1-VC + VN-SKL, HIS4, AMP*$_R$	This study
pPL18	P_{HTX1}-*MDHA-VC + VN-SKL, HIS4, AMP*$_R$	This study
pPL19	P_{HTX1}-*MDHB-VC + VN-SKL, HIS4, AMP*$_R$	This study
pPL20	P_{HTX1}-*GPDA-VC + VN-SKL, HIS4, AMP*$_R$	This study
pPL21	P_{HTX1}-*GAPDH-VC + VN-SKL, HIS4, AMP*$_R$	This study
pPL23	P_{HTX1}-*VC-MDHB + VN-SKL, HIS4, AMP*$_R$	This study
pPL26	P_{AOX1}-*MDHB-GFP, HIS4, AMP*$_R$	This study
pJCF235-ZEO	P_{PEX3}-*PEX3-mRFP, Zeocin*$_R$*, AMP*$_R$	Lab stock

Yeast Media

YPD (2% glucose, 2% bacto-peptone, 1% yeast extract), YNB (0.17% yeast nitrogen base without amino acids and ammonium sulfate, 0.5% ammonium sulfate), CSM (complete synthetic medium of amino acids and supplements), oleate medium (2x YNB, 0.79g/L CSM, 0.04 mg/L biotin, 0.02% Tween-40, 0.2% oleate), methanol medium (2x YNB, 0.79g/L CSM, 0.04 mg/L biotin, 0.5% methanol).

Plasmid Construction

Plasmids were constructed by Gibson Assembly. Gibson assembly primers were designed using NEBuilder (https://nebuilder.neb.com/#!/). DNA was amplified from wild-type genomic DNA by PCR using Advantage 2 Polymerase (Clontech Takara). Plasmid backbones were double digested with the necessary restriction enzymes and purified using the Qiagen DNA purification kit. DNA inserts were cloned into the digested vectors using the NEBuilder Hifi DNA Assembly Mastermix (New England Biolabs) and incubated for 1h at 50°C. Newly assembled plasmids were transformed into GC10 chemically competent *E.coli*. 2µl of the Gibson Assembly mixture was added to the 50µl GC10 competent cells, put on ice for 30 min, heat shocked for 30 seconds at 42°C, placed on ice for 2 min, and then 950µl of S.O.C. medium was added. The mixture was

incubated at 37°C for 1h shaking at 250 rpm and then plated on LB plates with the appropriate antibiotic. Colonies were screened by colony PCR and positive colonies were cultured in 5ml of LB+antibiotic overnight. Plasmids were purified using the Wizard Miniprep Kit (Promega) and sequenced by Eton Bioscience.

Yeast Strain Construction

Plasmids were linearized with the appropriate restriction enzyme before transforming into yeast competent cells. Yeast strains were made competent by electroporation. Yeast strains were cultured in a 250ml flask with 50ml of YPD shaking at 250 rpm at 30°C and grown until 1-2 OD_{600}/ml (exponential phase). Cells were pelleted by centrifugation at 3000 rpm for 3 min and resuspended in 5ml of YPD, 100µl of 1M HEPES (pH 8), and 125µl of 1M DTT. The resuspended cells were incubated at 30°C for 15 min on a lab rotator and then washed three times with cold sterile water and once with 1M cold sorbitol. Cells were gently resuspended with 200-300µl of cold sorbitol and placed on ice for 1h. 50µl of cells and 5µl of linearized DNA were mixed together and transferred into a pre-chilled electroporation cuvette. After 10 min on ice, the mixture was electroporated using the BTX Harvard Apparatus Electroporator and was immediately resuspended in 1M cold sorbitol. The transformed cells were plated on YPD plates with the appropriate yeast selection markers and incubated at 30°C for a few days. Colonies were screened by Western Blot or fluorescence microscopy.

Fluorescence Microscopy

Cells were grown in YPD at 30°C until exponential phase (1-2 OD_{600}/ml), washed twice with sterile water, and then transferred to peroxisome proliferation media. Cells were grown in oleate

or methanol media overnight (16h) and washed twice with sterile water. Cells were then pelleted and 1.5µl of cells were placed on a glass slide with a cover slip. Fluorescence was imaged using the Carl Zeiss Axiovision Microscope.

Chapter 1 is co-authored with Farré, Jean-Claude. The thesis author was the primary author of this chapter.

References

Agrawal, Gaurav, and Suresh Subramani. “Emerging Role of the Endoplasmic Reticulum in Peroxisome Biogenesis.” *Frontiers in Physiology*, vol. 4 OCT, no. October, 2013, pp. 1–8, doi:10.3389/fphys.2013.00286.

Al-Saryi, Nadal A., Murtakab Y. Al-Hejjaj, Carlo W. T. Van Roermund, Georgia E. Hulmes, Lakhan Ekal, Chantell Payton, Ronald J. A. Wanders, and Ewald H. Hettema. “Two NAD-Linked Redox Shuttles Maintain the Peroxisomal Redox Balance in *Saccharomyces Cerevisiae*.” *Scientific Reports*, 2017, doi:10.1038/s41598-017-11942-2.

Ast, Julia, Alina C. Stiebler, Johannes Freitag, and Michael Bölker. “Dual Targeting of Peroxisomal Proteins.” *Frontiers in Physiology*, vol. 4, no. October, 2013, pp. 1–8, doi:10.3389/fphys.2013.00297.

Baertling, F., L. Sánchez-Caballero, M. A. M. van den Brand, C. W. Fung, S. H. S. Chan, V. C. N. Wong, D. M. E. Hellebrekers, I. F. M. de Coo, J. A. M. Smeitink, R. J. T. Rodenburg, and L. G. J. Nijtmans. “NDUFA9 Point Mutations Cause a Variable Mitochondrial Complex I Assembly Defect.” *Clinical Genetics*, vol. 93, no. 1, 2018, pp. 111–18, doi:10.1111/cge.13089.

Bakker, Barbara M., Karin M. Overkamp, Antonius J. A. Van Maris, Peter Kötter, Marijke A. H. Luttik, Johannes P. Van Dijken, and Jack T. Pronk. “Stoichiometry and Compartmentation of NADH Metabolism in *Saccharomyces Cerevisiae*.” *FEMS Microbiology Reviews*, vol. 25, no. 1, 2001, pp. 15–37, doi:10.1016/S0168-6445(00)00039-5.

Brocard, Cécile, and Andreas Hartig. “Peroxisome Targeting Signal 1: Is It Really a Simple Tripeptide?” *Biochimica et Biophysica Acta - Molecular Cell Research*, vol. 1763, no. 12, 2006, pp. 1565–73, doi:10.1016/j.bbamcr.2006.08.022.

Cavero, S., A. Vozza, A. Del Arco, L. Palmieri, A. Villa, E. Blanco, M. J. Runswick, J. E. Walker, S. Cerdán, F. Palmieri, and J. Satrústegui. “Identification and Metabolic Role of the Mitochondrial Aspartate-Glutamate Transporter in Saccharomyces Cerevisiae.” *Molecular Microbiology*, vol. 50, no. 4, 2003, pp. 1257–69, doi:10.1046/j.1365-2958.2003.03742.x.

Chen, Shun-Jia, Xia Wu, Brandon Wadas, Jang-Hyun Oh, and Alexander Varshavsky. “An N-End Rule Pathway That Recognizes Proline and Destroys Gluconeogenic Enzymes.” *Science*, vol. 355, no. 6323, Jan. 2017, p. eaal3655, doi:10.1126/science.aal3655.

Claros, Manuel G., and Pierre Vincens. “Computational Method to Predict Mitochondrially Imported Proteins and Their Targeting Sequences.” *European Journal of Biochemistry*, vol. 241, no. 3, 1996, pp. 779–86, doi:10.1111/j.1432-1033.1996.00779.x.

DeLoache, William C., Zachary N. Russ, and John E. Dueber. “Towards Repurposing the Yeast Peroxisome for Compartmentalizing Heterologous Metabolic Pathways.” *Nature Communications*, vol. 7, Nature Publishing Group, 2016, doi:10.1038/ncomms11152.

Distel, B., M. Veenhuis, and H. F. Tabak. “Import of Alcohol Oxidase into Peroxisomes of Saccharomyces Cerevisiae.” *The EMBO Journal*, vol. 6, no. 10, 1987, pp. 3111–16, doi:10.1002/j.1460-2075.1987.tb02620.x.

Elgersma, Y., C. W. van Roermund, R. J. Wanders, and H. F. Tabak. “Peroxisomal and Mitochondrial Carnitine Acetyltransferases of Saccharomyces Cerevisiae Are Encoded by a Single Gene.” *The EMBO Journal*, vol. 14, no. 14, 1995, pp. 3472–79, doi:10.1002/j.1460-2075.1995.tb07353.x.

Elgersma, Ype, Arnold Vos, Marlene Van den Berg, Carlo W. T. Van Roermund, Peter Van der Sluijs, Ben Distel, and Henk F. Tabak. “Analysis of the Carboxyl-Terminal Peroxisomal Targeting Signal 1 in a Homologous Context in Saccharomyces Cerevisiae.” *Journal of Biological Chemistry*, vol. 271, no. 42, 1996, pp. 26375–82, doi:10.1074/jbc.271.42.26375.

Elgersma, Ype, Minetta Elgersma-Hooisma, Thibaut Wenzel, J. Michael McCaffery, Marilyn G. Farquhar, and Suresh Subramani. “A Mobile PTS2 Receptor for Peroxisomal Protein Import in Pichia Pastoris.” *Journal of Cell Biology*, vol. 140, no. 4, 1998, pp. 807–20, doi:10.1083/jcb.140.4.807.

Erdmann, Ralf. “The Peroxisomal Targeting Signal of 3-oxoacyl-coA Thiolase from Saccharomyces Cerevisiae.” *Yeast*, vol. 10, no. 7, 1994, pp. 935–44, doi:10.1002/yea.320100708.

Farré, Jean-Claude, Shanmuga S. Mahalingam, Marco Proietto, and Suresh Subramani. “Peroxisome Biogenesis, Membrane Contact Sites, and Quality Control.” *EMBO Reports*, vol. 20, no. 1, 2019, p. e46864, doi:10.15252/embr.201846864.

Gould, S. J., G. A. Keller, N. Hosken, J. Wilkinson, and S. Subramani. “A Conserved Tripeptide Sorts Proteins to Peroxisomes.” *Journal of Cell Biology*, vol. 108, no. 5, 1989, pp. 1657–64, doi:10.1083/jcb.108.5.1657.

Hiltunen, J. Kalervo, Anu M. Mursula, Hanspeter Rottensteiner, Rik K. Wierenga, Alexander J. Kastaniotis, and Aner Gurvitz. “The Biochemistry of Peroxisomal β-Oxidation in the Yeast *Saccharomyces Cerevisiae*.” *FEMS Microbiology Reviews*, vol. 27, no. 1, 2003, pp. 35–64, doi:10.1016/S0168-6445(03)00017-2.

Hofhuis, Julia, Fabian Schueren, Christopher Nötzel, Thomas Lingner, Jutta Gärtner, Olaf Jahn, and Sven Thoms. “The Functional Readthrough Extension of Malate Dehydrogenase Reveals a Modification of the Genetic Code.” *Open Biology*, vol. 6, no. 11, 2016, doi:10.1098/rsob.160246.

Jung, Sunhee, Marcello Marelli, Richard A. Rachubinski, David R. Goodlett, and John D. Aitchison. “Dynamic Changes in the Subcellular Distribution of Gpd1p in Response to Cell Stress.” *Journal of Biological Chemistry*, vol. 285, no. 9, 2010, pp. 6739–49, doi:10.1074/jbc.M109.058552.

Kabran, Philomne, Tristan Rossignol, Claude Gaillardin, Jean Marc Nicaud, and Ccile Neuvglise. "Alternative Splicing Regulates Targeting of Malate Dehydrogenase in *Yarrowia Lipolytica*." *DNA Research*, vol. 19, no. 3, 2012, pp. 231–44, doi:10.1093/dnares/dss007.

Klein, André T. J., Marlene V. Van Den Berg, Gina Bottger, Henk F. Tabak, and Ben Distel. "*Saccharomyces Cerevisiae* Acyl-CoA Oxidase Follows a Novel, Non-PTS1, Import Pathway into Peroxisomes That Is Dependent on Pex5p." *Journal of Biological Chemistry*, vol. 277, no. 28, 2002, pp. 25011–19, doi:10.1074/jbc.M203254200.

Knoblach, Barbara, and Richard A. Rachubinski. "Reconstitution of Human Peroxisomal β-Oxidation in Yeast." *FEMS Yeast Research*, vol. 18, no. 8, 2018, pp. 1–6, doi:10.1093/femsyr/foy092.

Kumar, Sanjeev, Ritika Singh, Chris P. Williams, and Ida J. van der Klei. "Stress Exposure Results in Increased Peroxisomal Levels of Yeast Pnc1 and Gpd1, Which Are Imported via a Piggy-Backing Mechanism." *Biochimica et Biophysica Acta - Molecular Cell Research*, vol. 1863, no. 1, The Authors, 2016, pp. 148–56, doi:10.1016/j.bbamcr.2015.10.017.

Kunze, Markus, and Andreas Hartig. "Permeability of the Peroxisomal Membrane: Lessons from the Glyoxylate Cycle." *Frontiers in Physiology*, vol. 4 AUG, no. August, 2013, pp. 1–12, doi:10.3389/fphys.2013.00204.

Kunze, Markus, Friedrich Kragler, Maximilian Binder, Andreas Hartig, and Aner Gurvitz. "Targeting of Malate Synthase 1 to the Peroxisomes of *Saccharomyces Cerevisiae* Cells Depends on Growth on Oleic Acid Medium." *European Journal of Biochemistry*, vol. 269, no. 3, 2002, pp. 915–22, doi:10.1046/j.0014-2956.2001.02727.x.

Kunze, Markus, Itsara Pracharoenwattana, Steven M. Smith, and Andreas Hartig. "A Central Role for the Peroxisomal Membrane in Glyoxylate Cycle Function." *Biochimica et Biophysica Acta - Molecular Cell Research*, vol. 1763, no. 12, 2006, pp. 1441–52, doi:10.1016/j.bbamcr.2006.09.009.

Kunze, Markus, Naila Malkani, Sebastian Maurer-Stroh, Christoph Wiesinger, Johannes A. Schmid, and Johannes Berger. "Mechanistic Insights into PTS2-Mediated Peroxisomal Protein Import: The Co-Receptor PEX5L Drastically Increases the Interaction Strength between the Cargo Protein and the Receptor PEX7." *Journal of Biological Chemistry*, vol. 290, no. 8, 2015, pp. 4928–40, doi:10.1074/jbc.M114.601575.

Lee, Y. J., G. R. Jeschke, F. M. Roelants, J. Thorner, and B. E. Turk. "Reciprocal Phosphorylation of Yeast Glycerol-3-Phosphate Dehydrogenases in Adaptation to Distinct Types of Stress." *Molecular and Cellular Biology*, vol. 32, no. 22, 2012, pp. 4705–17, doi:10.1128/mcb.00897-12.

Ma, Changle, Gaurav Agrawal, and Suresh Subramani. "Peroxisome Assembly: Matrix and Membrane Protein Biogenesis." *Journal of Cell Biology*, vol. 193, no. 1, 2011, pp. 7–16,

doi:10.1083/jcb.201010022.

McAlister-Henn, L., and L. M. Thompson. “Isolation and Expression of the Gene Encoding Yeast Mitochondrial Malate Dehydrogenase.” *Journal of Bacteriology*, vol. 169, no. 11, 1987, pp. 5157–66, doi:10.1128/jb.169.11.5157-5166.1987.

McAlister-Henn, L., J. S. Steffan, K. I. Minard, and S. L. Anderson. “Expression and Function of a Mislocalized Form of Peroxisomal Malate Dehydrogenase (MDH3) in Yeast.” *Journal of Biological Chemistry*, vol. 270, no. 36, 1995, pp. 21220–25, doi:10.1074/jbc.270.36.21220.

McCollum, D., E. Monosov, and S. Subramani. “The Pas8 Mutant of *Pichia Pastoris* Exhibits the Peroxisomal Protein Import Deficiencies of Zellweger Syndrome Cells--the PAS8 Protein Binds to the COOH-Terminal Tripeptide Peroxisomal Targeting Signal, and Is a Member of the TPR Protein Family.” *The Journal of Cell Biology*, vol. 121, no. 4, May 1993, pp. 761–74, doi:10.1083/jcb.121.4.761.

Minard, K. I., and L. McAlister-Henn. “Glucose-Induced Degradation of the MDH2 Isozyme of Malate Dehydrogenase in Yeast.” *Journal of Biological Chemistry*, vol. 267, no. 24, 1992, pp. 17458–64.

Minard, K. I., and L. McAlister-Henn. “Isolation, Nucleotide Sequence Analysis, and Disruption of the MDH2 Gene from *Saccharomyces Cerevisiae*: Evidence for Three Isozymes of Yeast Malate Dehydrogenase.” *Molecular and Cellular Biology*, vol. 11, no. 1, 1991, pp. 370–80, doi:10.1128/mcb.11.1.370.

Moriyama, Shu, Kazuya Nishio, and Tsunehiro Mizushima. “Structure of Glyoxysomal Malate Dehydrogenase (MDH3) from *Saccharomyces Cerevisiae*.” *Acta Crystallographica Section F: Structural Biology Communications*, vol. 74, no. 10, International Union of Crystallography, 2018, pp. 617–24, doi:10.1107/S2053230X18011895.

Motley, Alison M., and Ewald H. Hettema. “Yeast Peroxisomes Multiply by Growth and Division.” *Journal of Cell Biology*, vol. 178, no. 3, 2007, pp. 399–410, doi:10.1083/jcb.200702167.

Nazarko, Taras Y., Jean-Claude Farré, and Suresh Subramani. “Peroxisome Size Provides Insights into the Function of Autophagy-Related Proteins.” *Molecular Biology of the Cell*, 2009/07/15, vol. 20, no. 17, The American Society for Cell Biology, Sept. 2009, pp. 3828–39, doi:10.1091/mbc.e09-03-0221.

Neuberger, Georg, Sebastian Maurer-Stroh, Birgit Eisenhaber, Andreas Hartig, and Frank Eisenhaber. “Prediction of Peroxisomal Targeting Signal 1 Containing Proteins from Amino Acid Sequence.” *Journal of Molecular Biology*, vol. 328, no. 3, 2003, pp. 581–92, doi:10.1016/S0022-2836(03)00319-X.

Oeljeklaus, Silke, Andreas Schummer, Thomas Mastalski, Harald W. Platta, and Bettina Warscheid. “Regulation of Peroxisome Dynamics by Phosphorylation.” *Biochimica et Biophysica Acta - Molecular Cell Research*, vol. 1863, no. 5, Elsevier B.V., 2016, pp. 1027–

37, doi:10.1016/j.bbamcr.2015.12.022.

Palmieri, Ferdinando, Gennaro Agrimi, Emanuela Blanco, Alessandra Castegna, Maria A. Di Noia, Vito Iacobazzi, Francesco M. Lasorsa, Carlo M. T. Marobbio, Luigi Palmieri, Pasquale Scarcia, Simona Todisco, Angelo Vozza, and John Walker. "Identification of Mitochondrial Carriers in *Saccharomyces Cerevisiae* by Transport Assay of Reconstituted Recombinant Proteins." *Biochimica et Biophysica Acta - Bioenergetics*, vol. 1757, no. 9–10, 2006, pp. 1249–62, doi:10.1016/j.bbabio.2006.05.023.

Pines, O., S. Shemesh, E. Battat, and I. Goldberg. "Overexpression of Cytosolic Malate Dehydrogenase (MDH2) Causes Overproduction of Specific Organic Acids in *Saccharomyces Cerevisiae*." *Applied Microbiology and Biotechnology*, vol. 48, no. 2, 1997, pp. 248–55, doi:10.1007/s002530051046.

Poirier, Yves, Vasily D. Antonenkov, Tuomo Glumoff, and J. Kalervo Hiltunen. "Peroxisomal β-Oxidation-A Metabolic Pathway with Multiple Functions." *Biochimica et Biophysica Acta - Molecular Cell Research*, vol. 1763, no. 12, 2006, pp. 1413–26, doi:10.1016/j.bbamcr.2006.08.034.

Saryi, Nadal A. A., John D. Hutchinson, Murtakab Y. Al-Hejjaj, Svetlana Sedelnikova, Patrick Baker, and Ewald H. Hettema. "Pnc1 Piggy-Back Import into Peroxisomes Relies on Gpd1 Homodimerisation." *Scientific Reports*, vol. 7, no. August 2016, Nature Publishing Group, 2017, pp. 1–12, doi:10.1038/srep42579.

Schueren, Fabian, Thomas Lingner, Rosemol George, Julia Hofhuis, Corinna Dickel, Jutta Gärtner, and Sven Thoms. "Peroxisomal Lactate Dehydrogenase Is Generated by Translational Readthrough in Mammals." *ELife*, vol. 3, 2014, p. e03640, doi:10.7554/eLife.03640.

Shyu, Y. John, Christopher D. Suarez, and Chang Deng Hu. "Visualization of Ternary Complexes in Living Cells by Using a BiFC-Based FRET Assay." *Nature Protocols*, vol. 3, no. 11, 2008, pp. 1693–702, doi:10.1038/nprot.2008.157.

Steffan, J. S., and L. McAlister-Henn. "Isolation and Characterization of the Yeast Gene Encoding the MDH3 Isozyme of Malate Dehydrogenase." *Journal of Biological Chemistry*, vol. 267, no. 34, 1992, pp. 24708–15.

Stiebler, Alina C., Johannes Freitag, Kay O. Schink, Thorsten Stehlik, Britta A. M. Tillmann, Julia Ast, and Michael Bölker. "Ribosomal Readthrough at a Short UGA Stop Codon Context Triggers Dual Localization of Metabolic Enzymes in Fungi and Animals." *PLoS Genetics*, vol. 10, no. 10, 2014, pp. 1–9, doi:10.1371/journal.pgen.1004685.

Thomas, Ann S., Arjen M. Krikken, Rinse de Boer, and Chris Williams. "*Hansenula Polymorpha* Aat2p Is Targeted to Peroxisomes via a Novel Pex20p-Dependent Pathway." *FEBS Letters*, vol. 592, no. 14, 2018, pp. 2466–75, doi:10.1002/1873-3468.13168.

Thompson, L. M., and L. McAlister-Henn. "Dispensable Presequence for Cellular Localization

and Function of Mitochondrial Malate Dehydrogenase from Saccharomyces Cerevisiae." *Journal of Biological Chemistry*, vol. 264, no. 20, 1989, pp. 12091–96.

Valadi, Åsa, Katarina Granath, Lena Gustafsson, and Lennart Adler. "Distinct Intracellular Localization of Gpd1p and Gpd2p, the Two Yeast Isoforms of NAD+-Dependent Glycerol-3-Phosphate Dehydrogenase, Explains Their Different Contributions to Redox-Driven Glycerol Production." *Journal of Biological Chemistry*, vol. 279, no. 38, 2004, pp. 39677–85, doi:10.1074/jbc.M403310200.

Van der Klei, Ida J., Hiroya Yurimoto, Yasuyoshi Sakai, and Marten Veenhuis. "The Significance of Peroxisomes in Methanol Metabolism in Methylotrophic Yeast." *Biochimica et Biophysica Acta - Molecular Cell Research*, vol. 1763, no. 12, 2006, pp. 1453–62, doi:10.1016/j.bbamcr.2006.07.016.

Van Roermund, C. W. T., H. R. Waterham, L. Ijlst, and R. J. A. Wanders. "Fatty Acid Metabolism in *Saccharomyces Cerevisiae*." *Cellular and Molecular Life Sciences*, vol. 60, no. 9, 2003, pp. 1838–51, doi:10.1007/s00018-003-3076-x.

Van Roermund, C. W., Y. Elgersma, N. Singh, R. J. Wanders, and H. F. Tabak. "The Membrane of Peroxisomes in *Saccharomyces Cerevisiae* Is Impermeable to NAD(H) and Acetyl-CoA under in Vivo Conditions." *The EMBO Journal*, vol. 14, no. 14, 1995, pp. 3480–86, doi:10.1002/j.1460-2075.1995.tb07354.x.

Veenhuis, M., J. P. Va. Dijken, and W. Harder. "The Significance of Peroxisomes in the Metabolism of One-Carbon Compounds in Yeasts." *Advances in Microbial Physiology*, vol. 24, no. C, 1983, doi:10.1016/S0065-2911(08)60384-7.

Verleur, Nicolette, Ype Elgersma, Carlo W. T. Van Roermund, Henk F. Tabak, and Ronald J. A. Wanders. "Cytosolic Aspartate Aminotransferase Encoded by the AAT2 Gene Is Targeted to the Peroxisomes in Oleate-Grown *Saccharomyces Cerevisiae*." *European Journal of Biochemistry*, vol. 247, no. 3, 1997, pp. 972–80, doi:10.1111/j.1432-1033.1997.00972.x.

Vogl, Thomas, Lukas Sturmberger, Thomas Kickenweiz, Richard Wasmayer, Christian Schmid, Anna Maria Hatzl, Michaela A. Gerstmann, Julia Pitzer, Marlies Wagner, Gerhard G. Thallinger, Martina Geier, and Anton Glieder. "A Toolbox of Diverse Promoters Related to Methanol Utilization: Functionally Verified Parts for Heterologous Pathway Expression in *Pichia Pastoris*." *ACS Synthetic Biology*, vol. 5, no. 2, 2016, pp. 172–86, doi:10.1021/acssynbio.5b00199.

Wanders, Ronald J. A., Hans R. Waterham, and Sacha Ferdinandusse. "Metabolic Interplay between Peroxisomes and Other Subcellular Organelles Including Mitochondria and the Endoplasmic Reticulum." *Frontiers in Cell and Developmental Biology*, vol. 3, no. JAN, 2016, pp. 1–15, doi:10.3389/fcell.2015.00083.

Yasokawa, Daisuke, Satomi Murata, Yumiko Iwahashi, Emiko Kitagawa, Ryoji Nakagawa, Tazusa Hashido, and Hitoshi Iwahashi. "Toxicity of Methanol and Formaldehyde towards

Saccharomyces Cerevisiae as Assessed by DNA Microarray Analysis." *Applied Biochemistry and Biotechnology*, vol. 160, no. 6, 2010, pp. 1685–98, doi:10.1007/s12010-009-8684-y.